The Abdus Salam
International Centre for Theoretical Physics

United Nations
Educational, Scientific and
Cultural Organization

IAEA
International Atomic Energy Agency

2272-5

Joint ICTP-IAEA School on Synchrotron Applications in Cultural Heritage and Environmental Sciences and Multidisciplinary Aspects of Imaging Techniques

21 - 25 November 2011

A Deep View in Cultural Heritage - Confocal Micro-XRF Spectroscopy for 3D elemental imaging and Analysis

Andreas - Germanos Karydas
IAEA, Vienna
Austria

A Deep View in Cultural Heritage - Confocal Micro-XRF Spectroscopy for 3D elemental imaging and Analysis

A.G. Karydas,
Nuclear Spectrometry and Applications Laboratory
IAEA Laboratories, Seibersdorf

X-rays Optics

Refractive index $\Rightarrow \quad n = \dfrac{c}{u_p}$

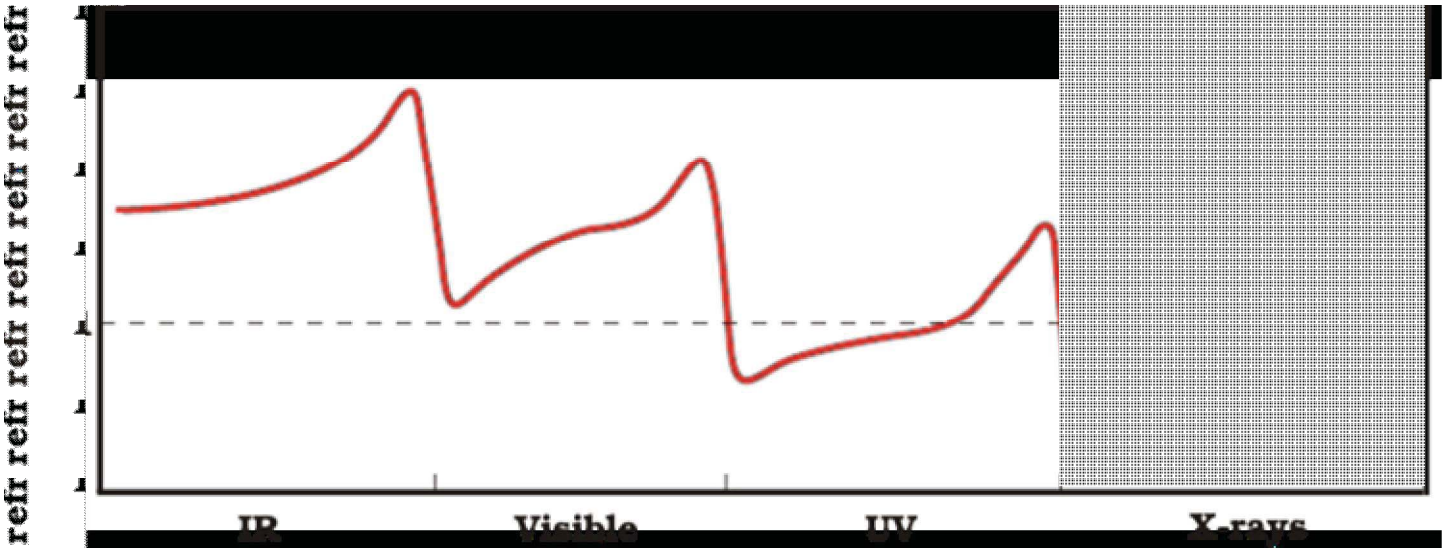

$$n = 1 - \delta - i\beta$$

$$\delta = \frac{414.7}{\mathrm{E}^2} \cdot \frac{\mathrm{Z}_\rho \cdot \rho}{\mathrm{A}}$$

phase term

$$\beta = \frac{\lambda}{4\pi}\tau$$

attenuation term

X-Ray optics: External total reflection

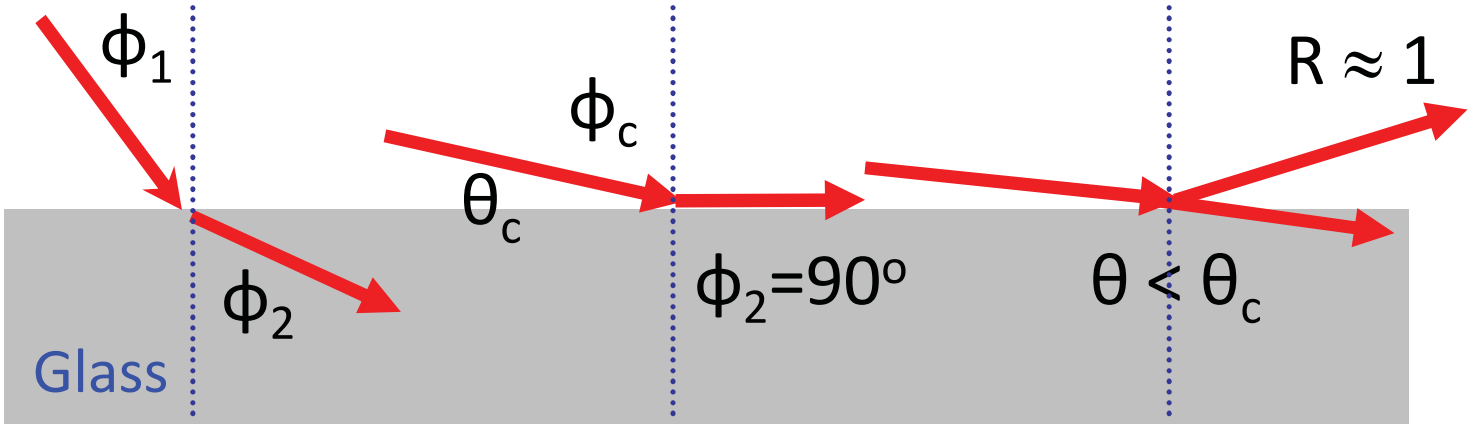

Snell Law: $\sin\varphi_2 = \frac{\sin\varphi_1}{n} \Rightarrow \varphi_2 > \varphi_1$

$$\theta_c = \sqrt{2\delta} = \frac{28.8}{E} \cdot \sqrt{\frac{Z_\rho \cdot \rho}{A}}$$

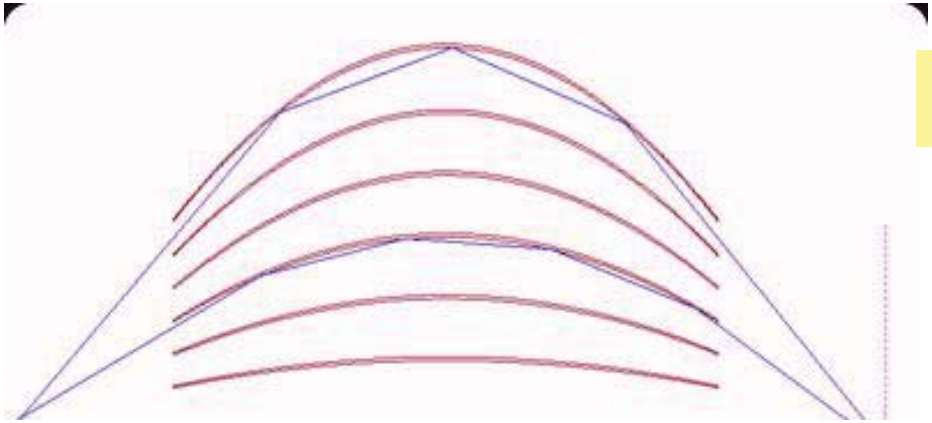

θ_c in the mrad range

Polycapillary X-ray lenses

Bundles of thousands glass mono-capillaries:

- **Directing**
- **Focusing**
- **Parallelizing**

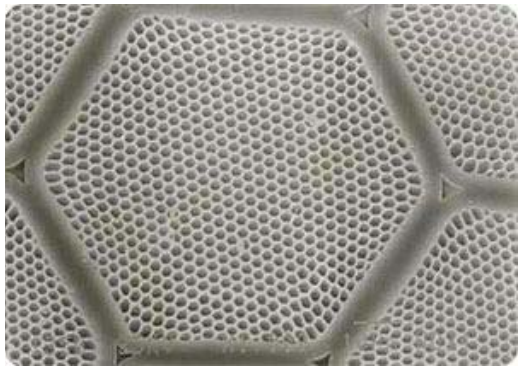

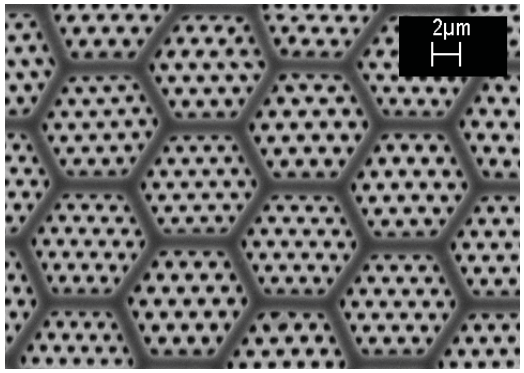

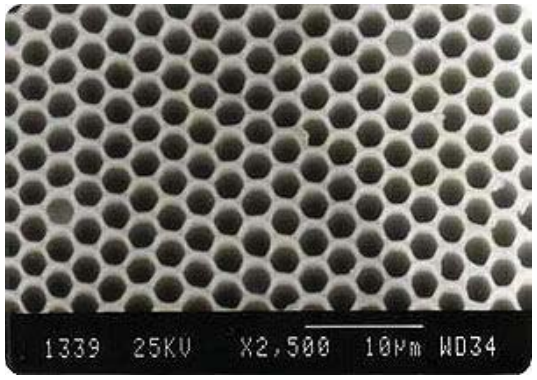

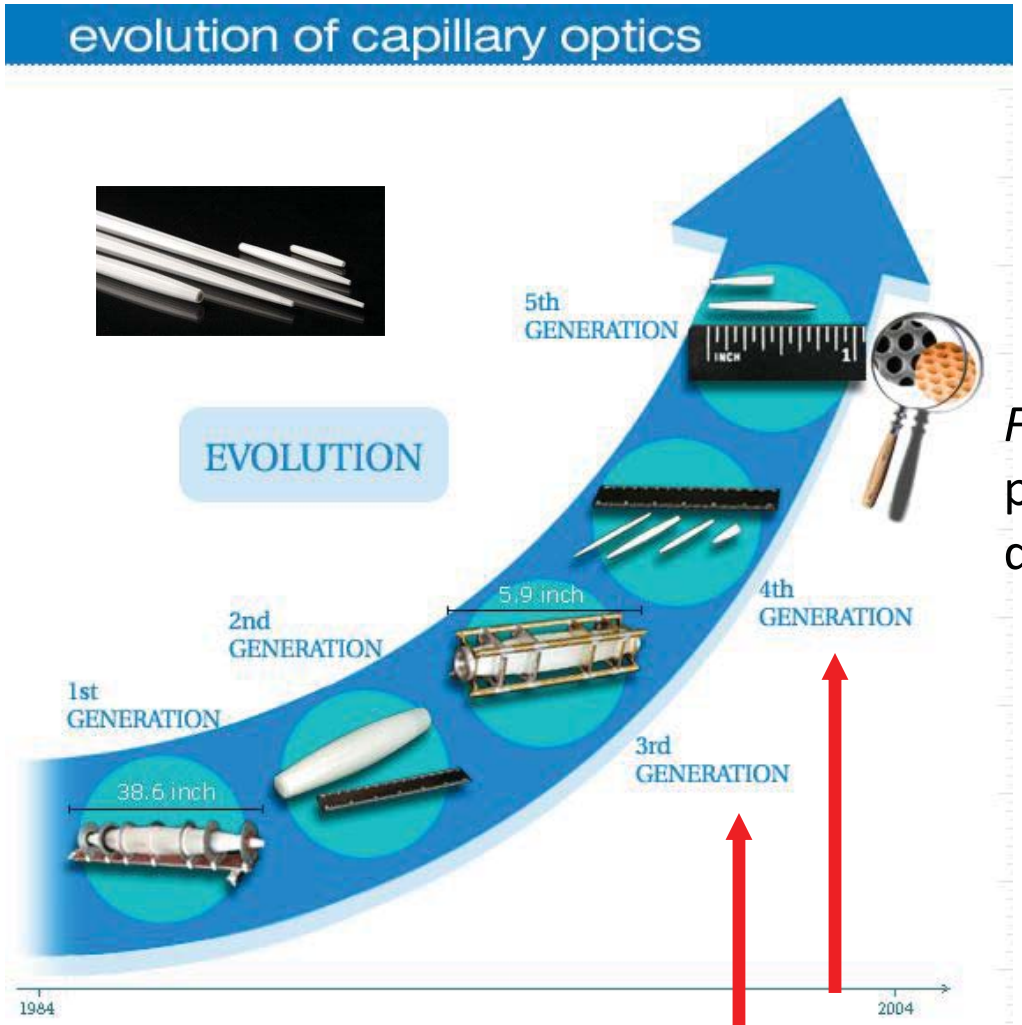

Polycapillary Semilens (half-lens)

Functionality: Spot focusing of parallel beam or conversion of a diverging beam to a parallel one.

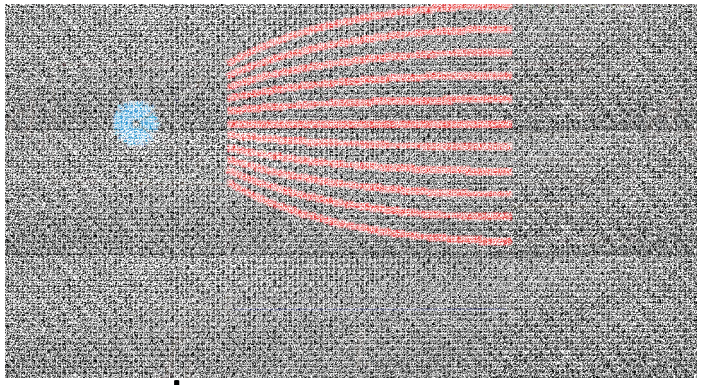

Assembled lens made of single capillaries

Monolithic integral Micro-lens

Monolithic lens, made of polycapillaries

Characteristics of X-Ray lenses

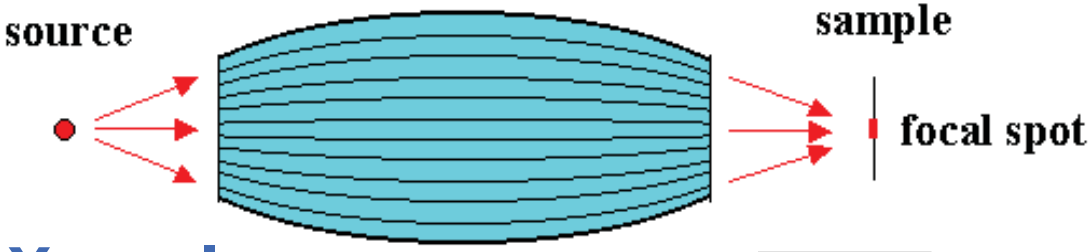

X-ray lens

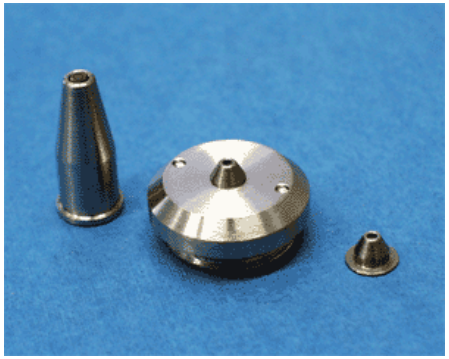

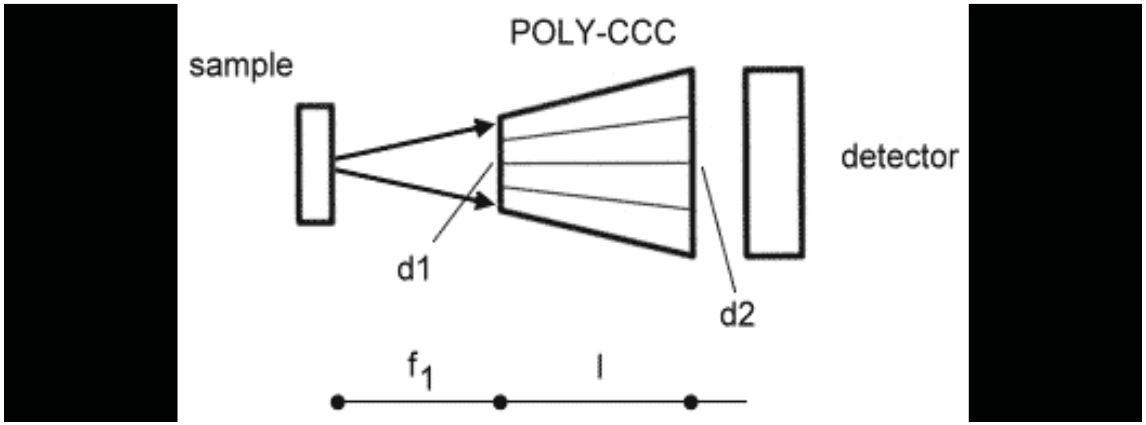

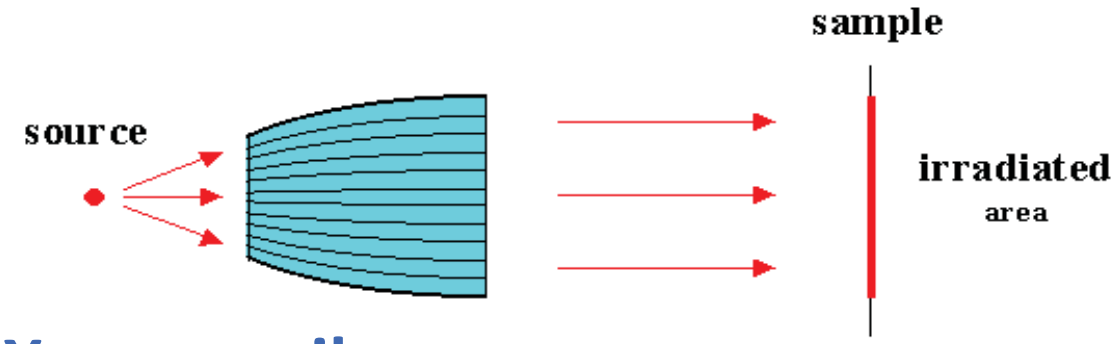

X-ray semilens

IAEA

Characteristics of polycappilary X-ray lenses

Important lens parameters:

- Focal distance (few mm).
- Size of the focal region represented by the FWHM of a Gaussian intensity distribution (down to ~ 12 um @ CuKα)

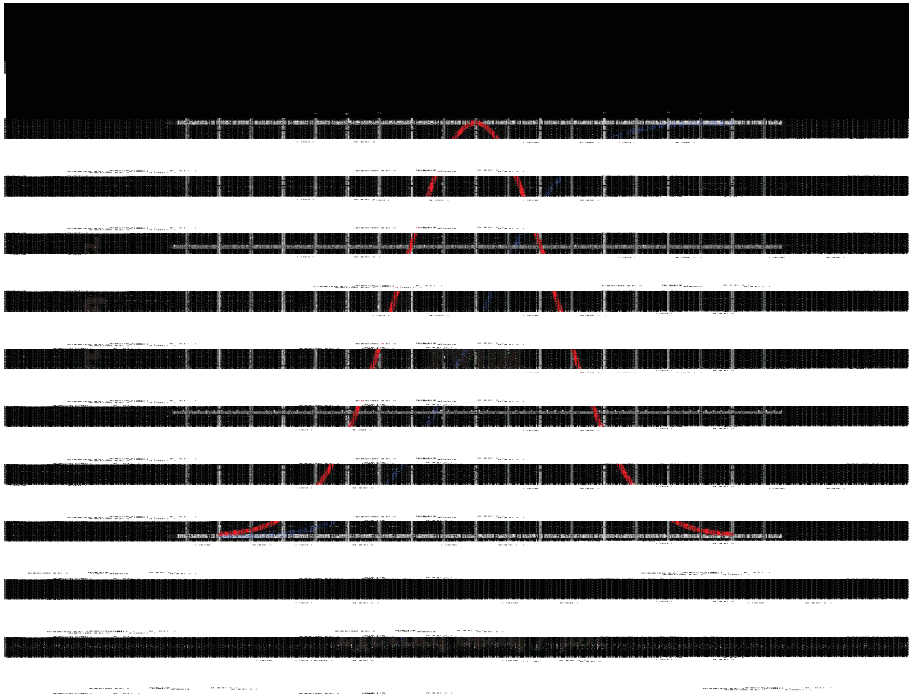

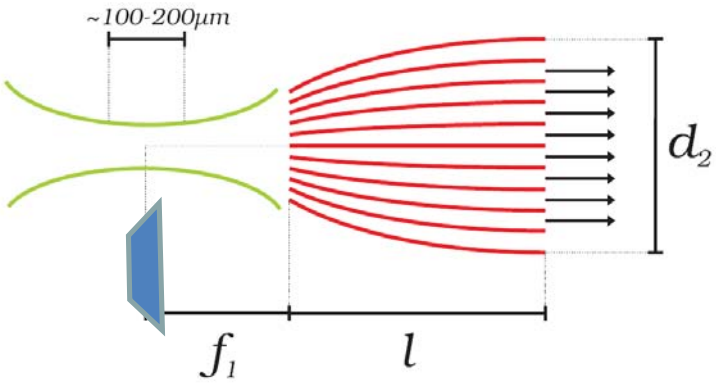

X-Ray lens spatial resolution

Plane vertical to the optical axis:
Two dimensional Gaussian

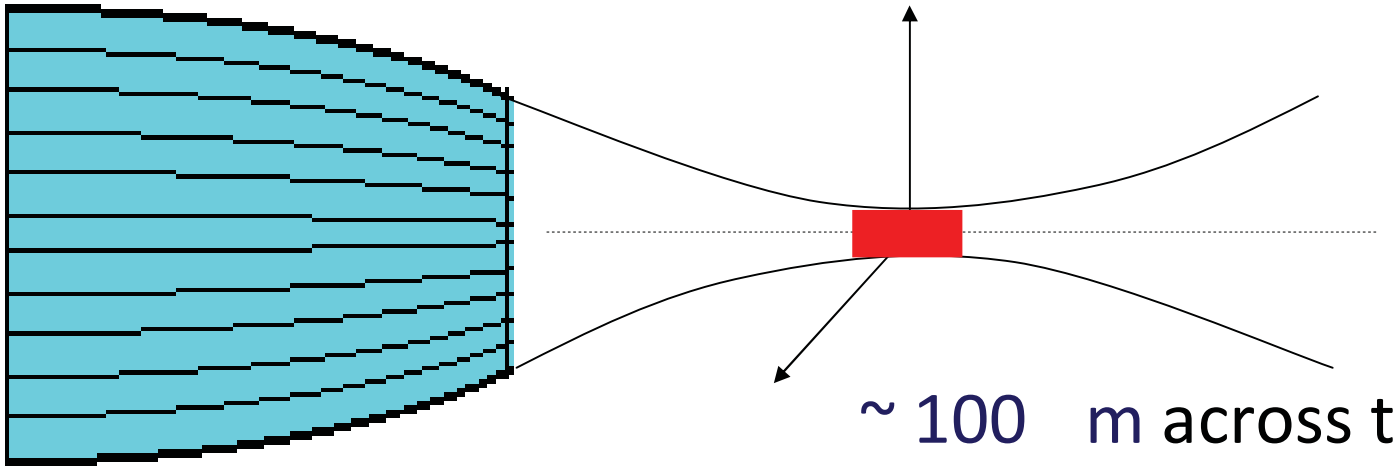

~ 100 m across the optical axis and the focal plane of the lens the spatial resolution remains constant

Principle of Confocal X-ray geometry

B. Kanngießer, I. Reiche, W. Malzer, NIM B 211, 2003

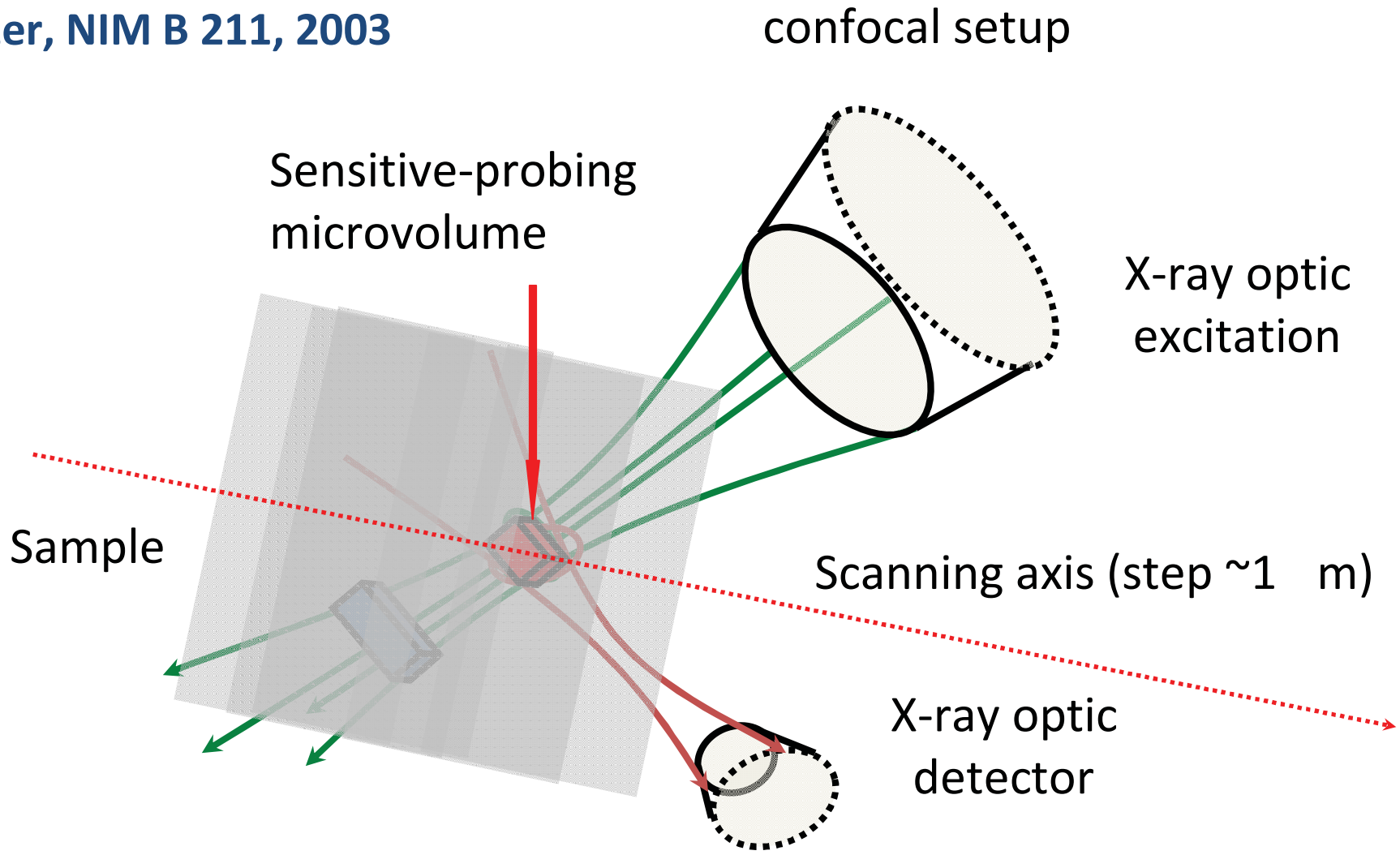

3D Micro XRF Spectrometry:

First setup of the 3D Micro-XRF, @ BAMline, BESSY

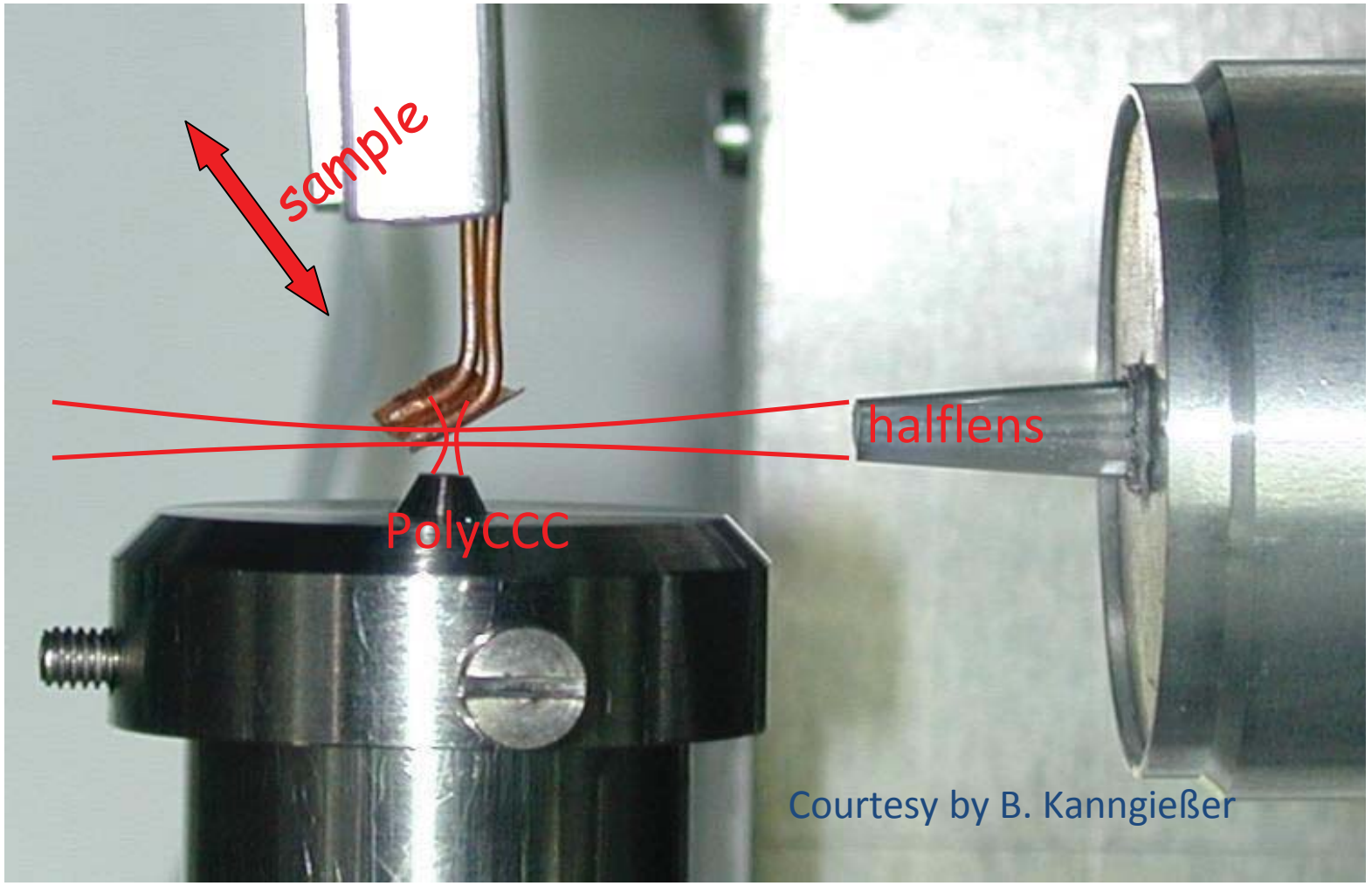

3D Micro–XRF setup: Synchrotron Radiation – Spot line, BESSY, Berlin

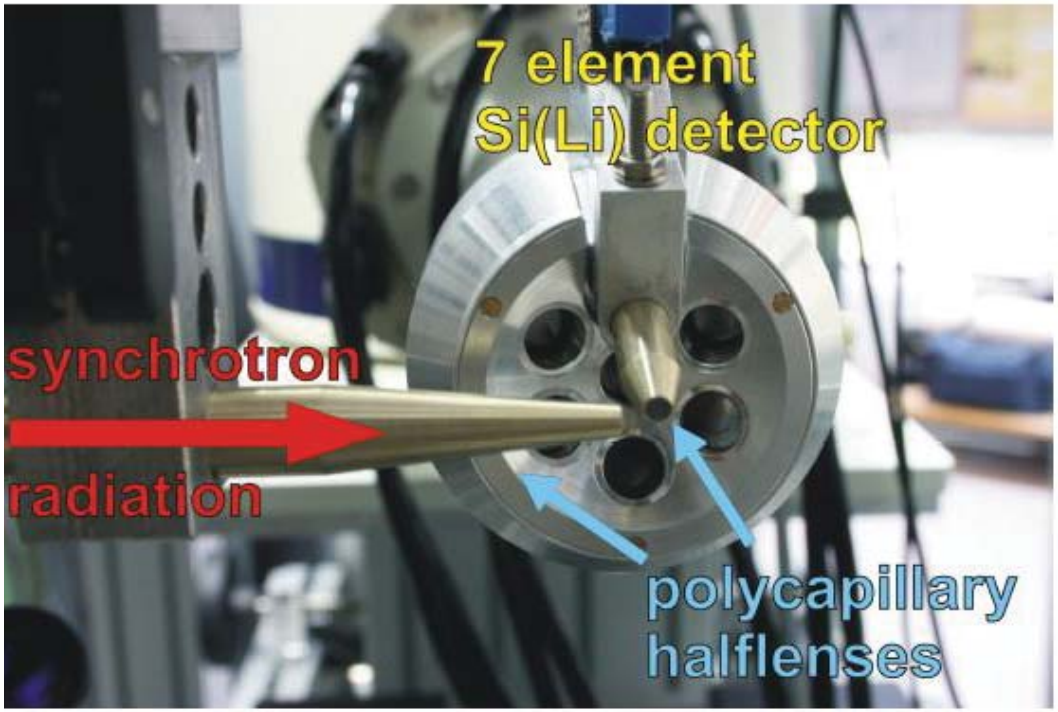

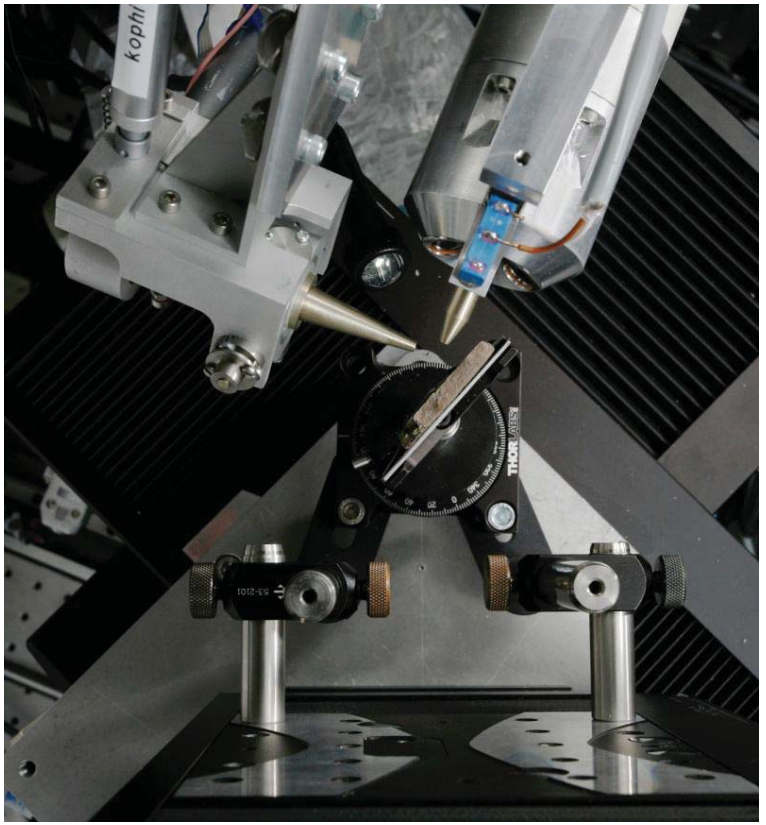

3D Micro–XRF setup @ TU Berlin

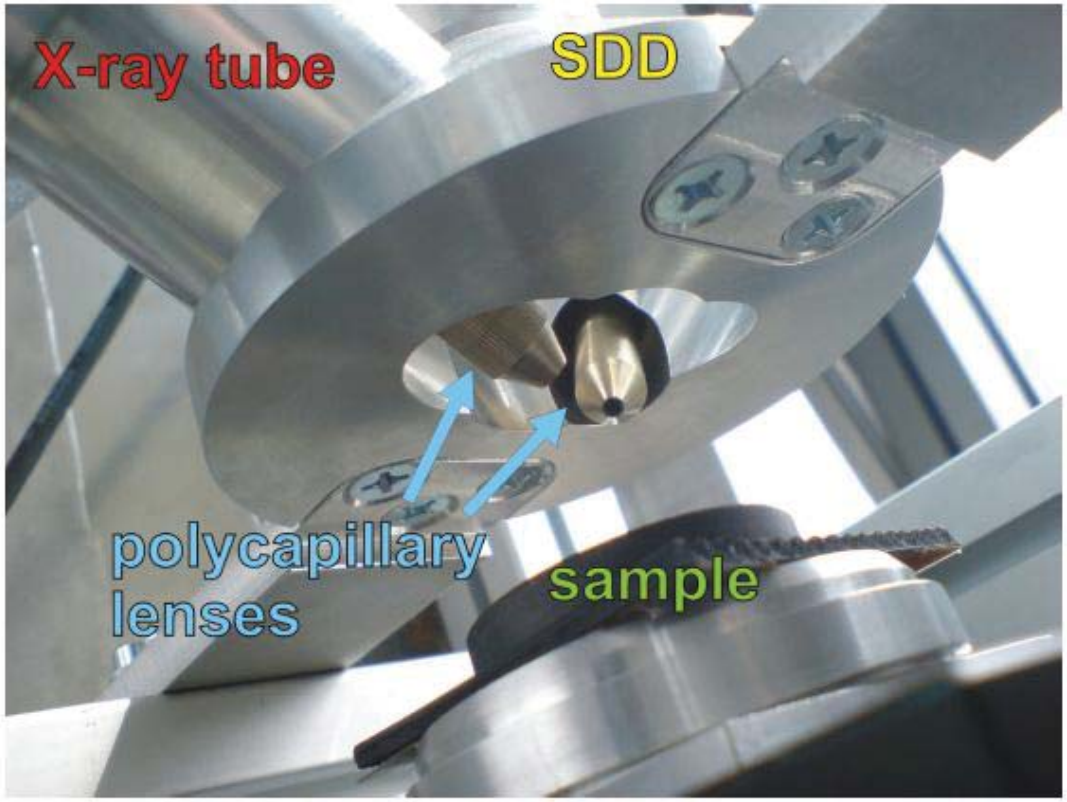

3D Micro–XRF setup @ IAEA, Seibersdorf

Spatial resolution:

15 - 40 mm

3 SDD's

DSP

3 stages:

Alignment-

Sample movement

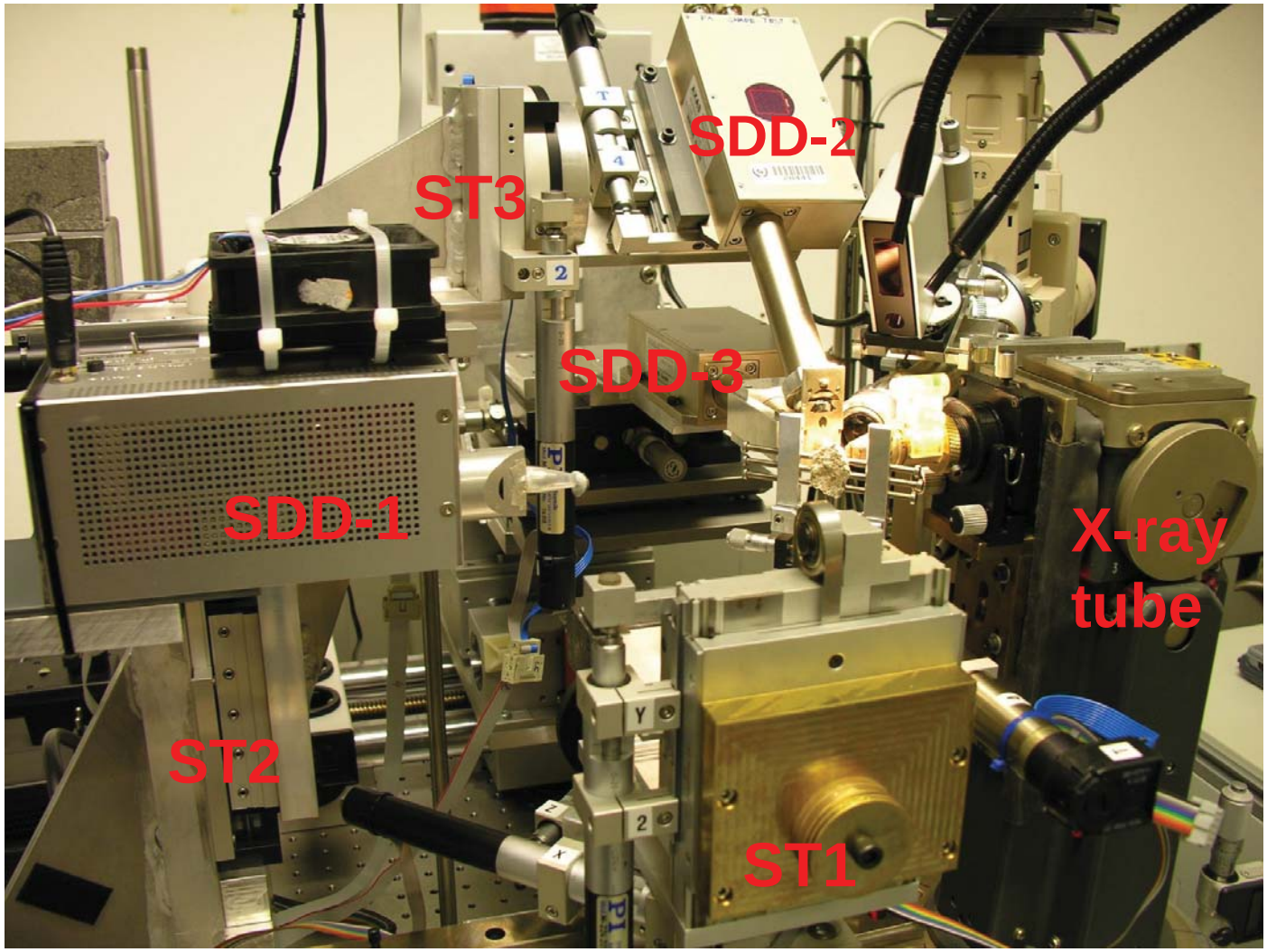

IAEA

3D uXRF set-up @IAEA

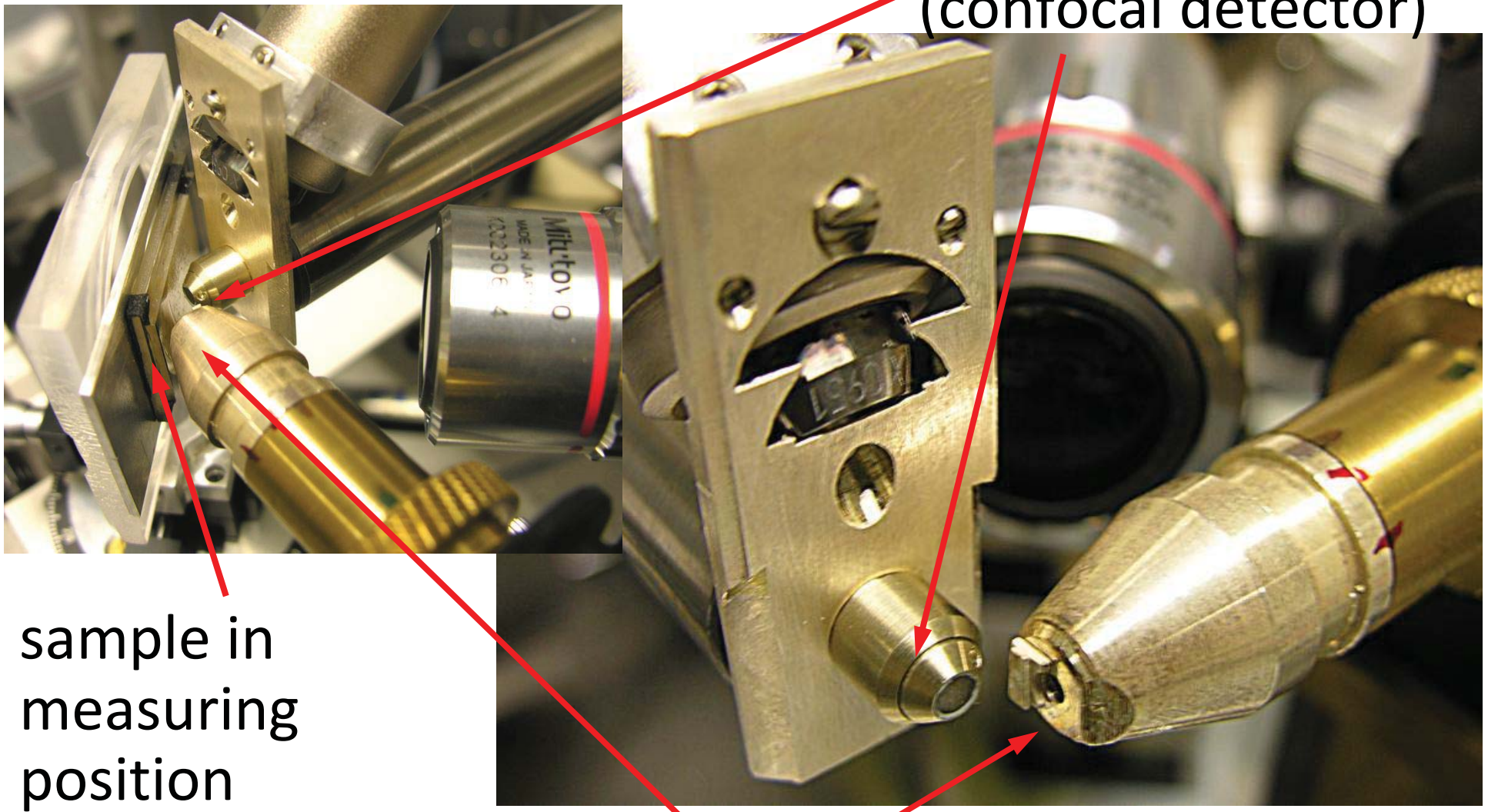

3D Micro-PIXE SET-UP, 2007 @

[redacted]-Analytical Center, Ljubljana

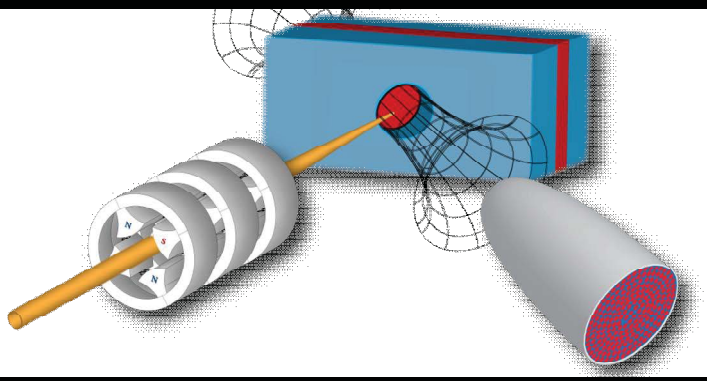

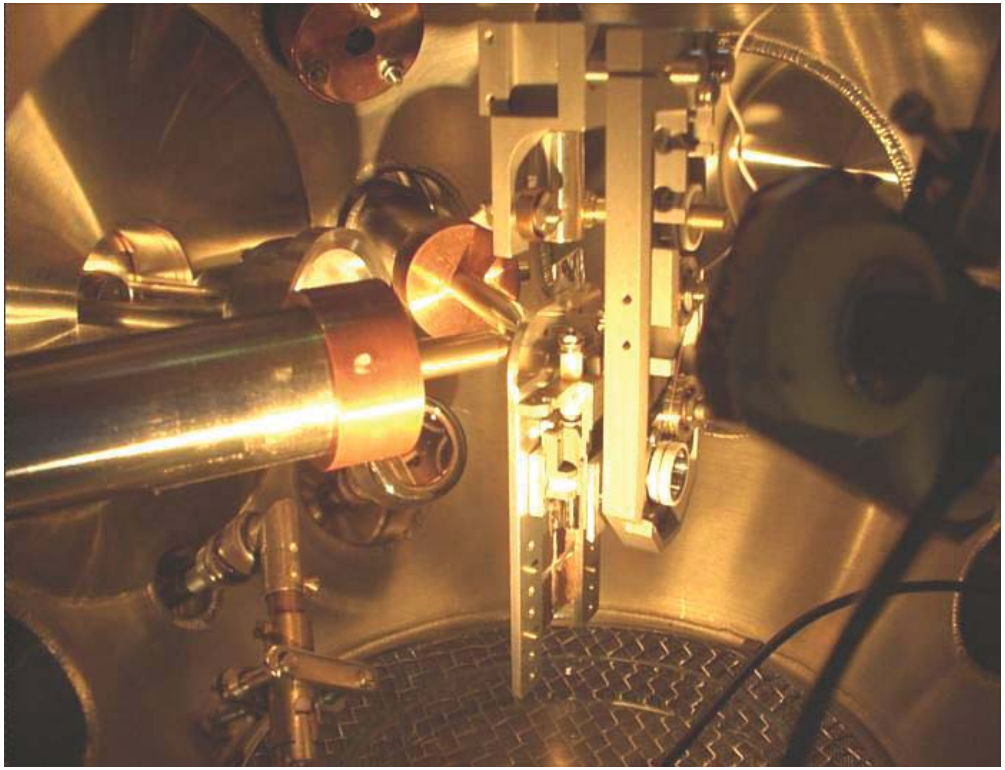

Basics in XRF Quantification

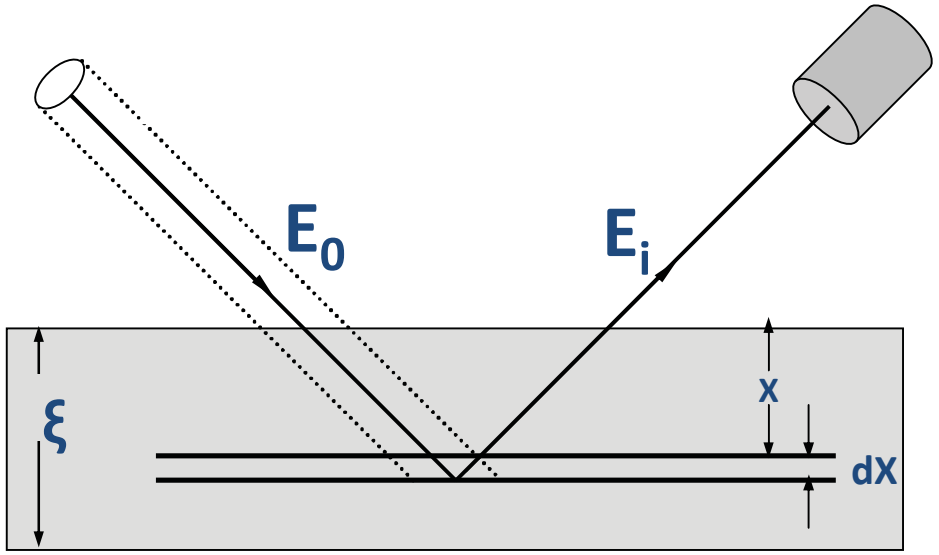

- ✓ Monochromatic excitation
- ✓ Homogeneous sample

$$\mu_s(E_o, E_i) = \sum_{k=1}^{n} c_k \cdot \left[\frac{\mu_k(E_0)}{\sin\theta_1} + \frac{\mu_k(E_i)}{\sin\theta_2} \right]$$

Geometrical Factor — Detector Efficiency

$$I_a(E_i) = I_o \cdot G \cdot \sigma_i^a(E_0) \cdot f_{ab}(E_i) \cdot \varepsilon_d(E_i) \cdot c_a \cdot \frac{1 - \exp\left[-\mu_s(E_o, E_i) \cdot \xi\right]}{\mu_s(E_i)}$$

Beam Intensity — Cross section — Air absorption — Analyte Concentration

Sensitivity constant

Quantification in Confocal Micro XRF (1)

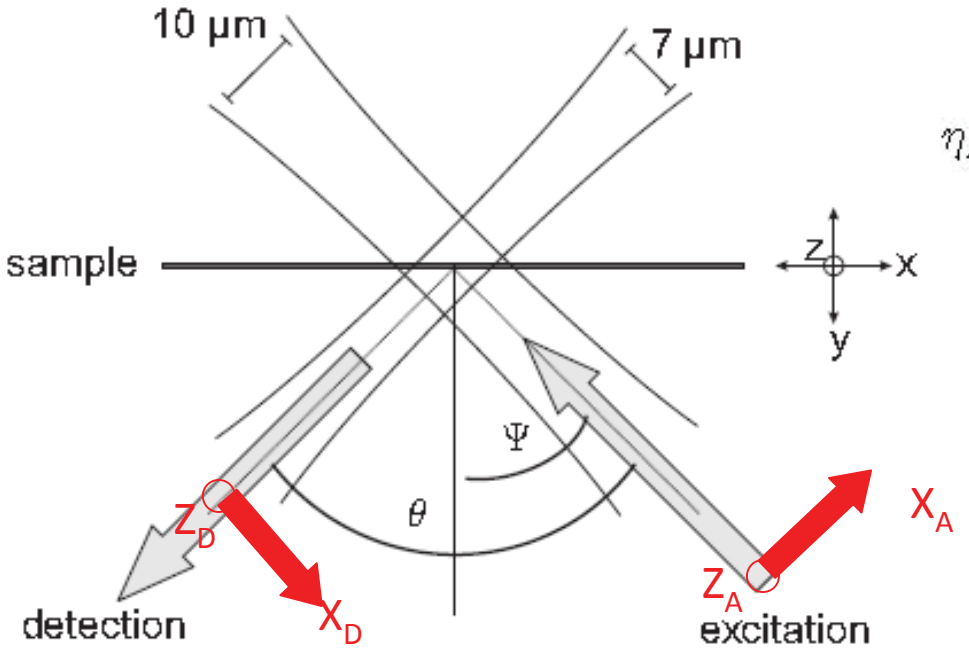

Intensity distribution for the exciting x-ray beam:

$$\eta_A = \frac{T_A}{2\pi\sigma_A^2}\exp\left(-\frac{x_A^2 + z_A^2}{2\sigma_A^2}\right)$$

Coordination system attached to the excitation lens

T_A, T_B: Lens transmission

σ_A, σ_B : Spot size

Ω **:** solid angle

$$\eta_D = \frac{\Omega T_D}{4\pi}\exp\left(-\frac{x_D^2 + z_D^2}{2\sigma_D^2}\right)$$

Coordination system attached to the detection lens

3D set-up sensitivity for the detection of specific fluorescence lines
The shape has a three dimensional **ellipsoid**

$$\hat{\eta}(x,y,z) = \eta_A \eta_D \epsilon = \frac{\Omega T_A T_D \epsilon}{8\pi^2\sigma_A^2}\exp\left(-\frac{\sigma_D^2 x_A^2 + \sigma_A^2 x_D^2 + (\sigma_D^2 + \sigma_A^2)z^2}{2\sigma_A^2\sigma_D^2}\right)$$

IAEA

Quantification in Confocal Micro XRF (2)

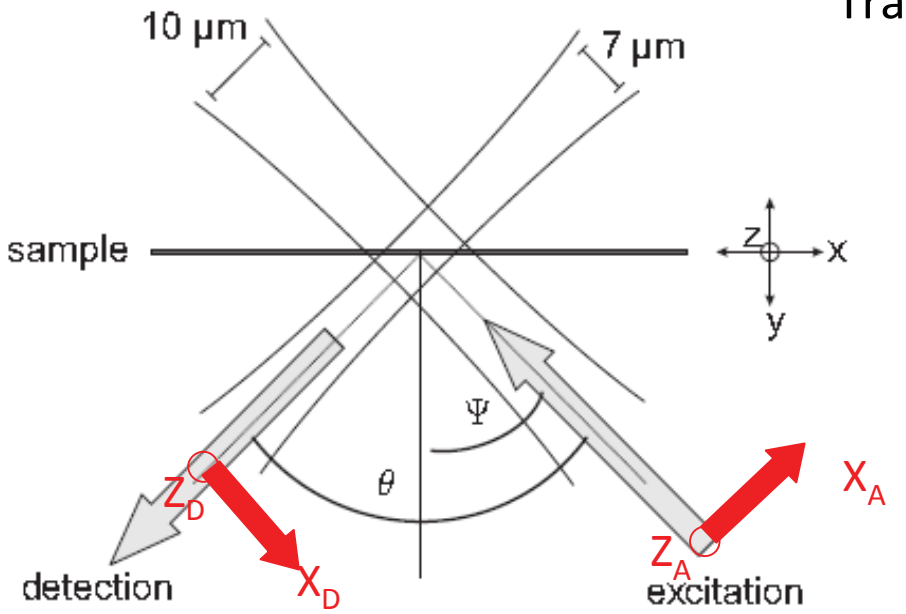

Transformation to the sample coordinate system

$$\begin{aligned} x_A &= x\sin(\Psi) + y\cos(\Psi) \\ x_D &= x\cos(\Psi) - y\sin\Psi \\ z_A &= z_D = z \end{aligned}$$

$$\tilde{\eta}(y) = \int_{-\infty}^{\infty}\int_{-\infty}^{\infty}\hat{\eta}(x,y,z)dxdz$$

$$= \frac{\Omega T_A T_D \epsilon}{4\pi}\frac{\sigma_D^2}{\sqrt{(\sigma_D^2+\sigma_A^2)(\cos^2(\Psi)\sigma_A^2+\sin^2(\Psi)\sigma_D^2)}}\exp\left(-\frac{1}{2}\frac{y^2}{(\sin^2(\Psi)\sigma_D^2+\cos^2(\Psi)\sigma_A^2)}\right)$$

Mantouvalou, PhD Thesis, Berlin 2009
Maltzer, kanngiesser, SAB 60 (2005) 1334 – 1341

$$= \frac{\eta}{\sqrt{2\pi}\sigma_y}\exp\left(-\frac{y^2}{2\sigma_y^2}\right)$$

Quantification in Confocal Micro XRF (3)

Fluorescence intensity in confocal geometry for an homogeneous sample

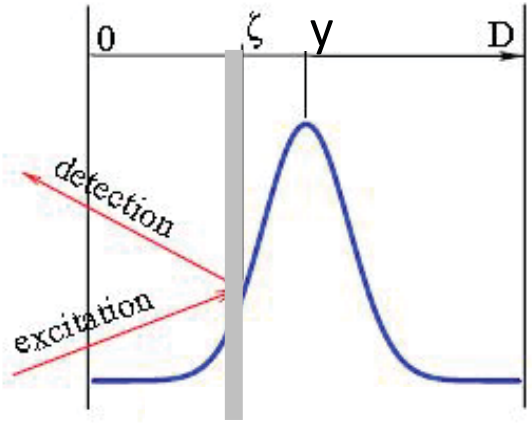

$$\Phi_i(y) = \Phi_o \cdot \sigma_{F.i} \int_o^D \overline{\eta}_i(\zeta - y)\,\rho_i(\zeta) \cdot \exp(-\overline{\mu}_{lin,i}\zeta) \cdot d\zeta$$

Local density of element *i*

$$\bar{\mu}_{lin,i} = \bar{\mu}_i \cdot \rho = \left(\sum_{elements\ j} \left(\frac{\mu_{0,j}}{\cos(\theta_A)} + \frac{\mu_{i,j}}{\cos(\theta_D)} \right) w_j \right) \rho$$

$$= \sum_{elements\ j} \left(\frac{\mu_{0,j}}{\cos(\theta_A)} + \frac{\mu_{i,j}}{\cos(\theta_D)} \right) \rho_j$$

$$\Phi_i(y) = \frac{\Phi_o \cdot \eta_i \cdot \rho_i \cdot \sigma_{F.i}}{2} \times \exp\left(\frac{\left(\overline{\mu}_{lin,i}\sigma_{y,i}\right)^2}{2} \right) \times \exp(-\overline{\mu}_{lin,i} y) \times$$

$$\times \left[erf\left(\frac{D + \overline{\mu}_{lin,i}\sigma_{y,i}^2 - y}{\sqrt{2}\sigma_{y,i}} \right) - erf\left(\frac{\overline{\mu}_{lin,i}\sigma_{y,i}^2 - y}{\sqrt{2}\sigma_{y,i}} \right) \right]_i$$

corrects for the actual extension of the probing volume

stands for the decrease of the intensity at probing depth x due to absorption.

important if the probing volume intersects the layer boundaries.

Shape of intensity profiles versus depth

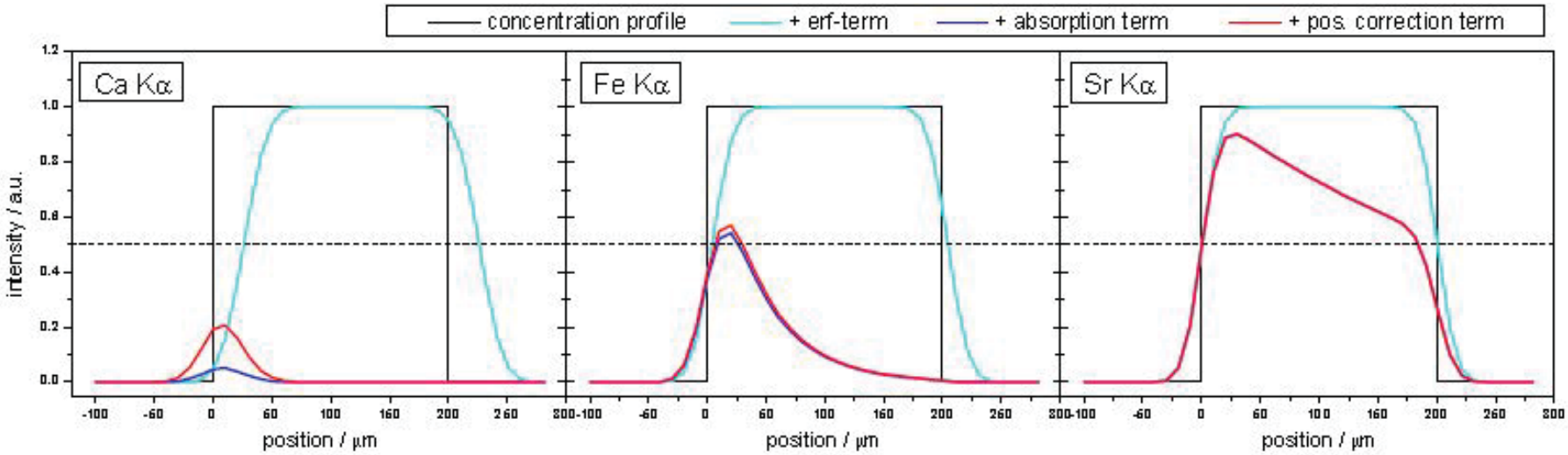

SiO_2 matrix, similar concentration (50 ppm), 19 keV excitation

I. Mantouvalou, PhD Thesis, Berlin 2009

Experimental FWHM, sensitivity/3D uXRF

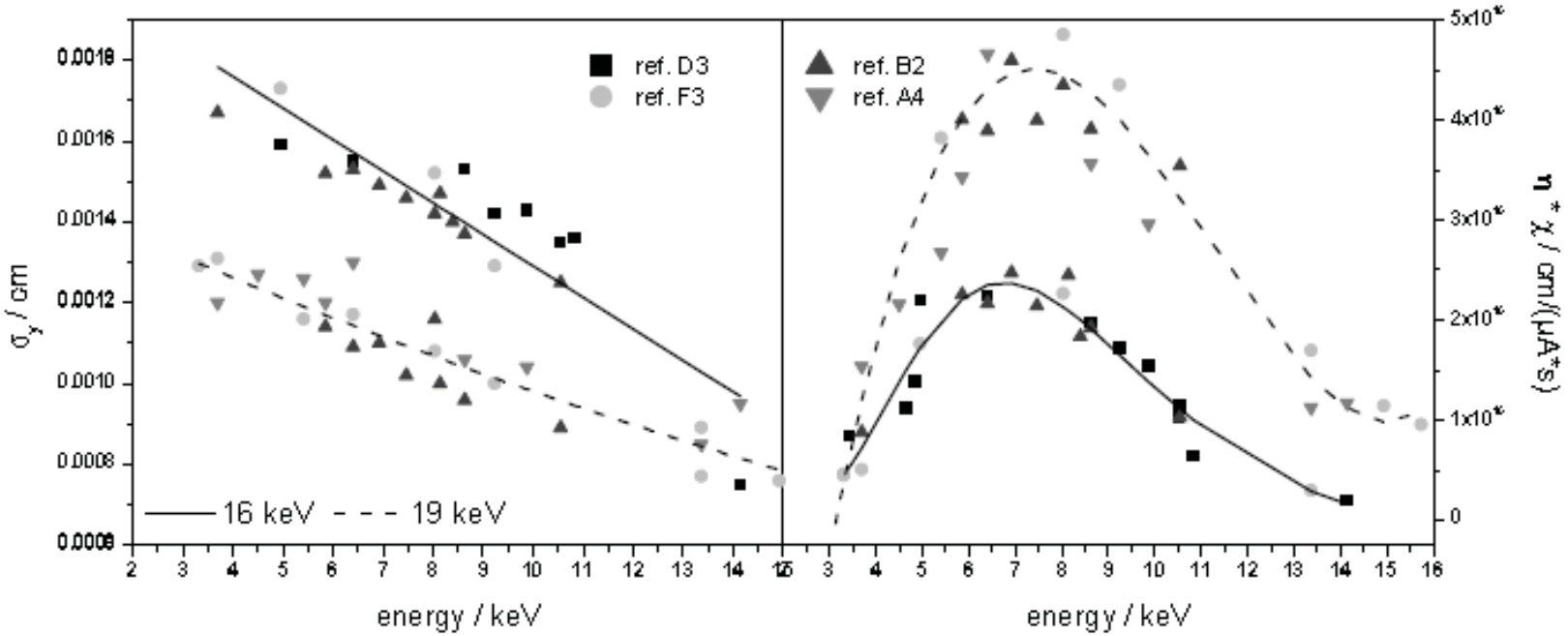

16, 19 keV excitation energies, Glass Reference materials

I. Mantouvalou, PhD Thesis, Berlin 2009

3D-uPIXE: Modeling the sensitive micro-volume

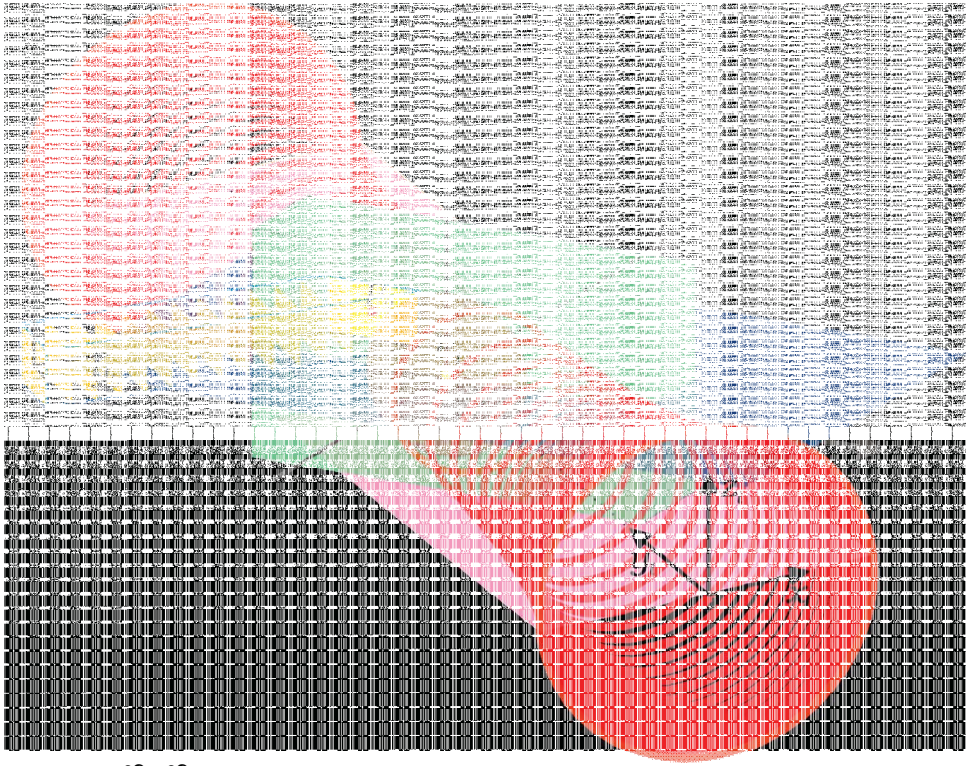

$$K(x_o, y, z_o) = \int_{-\infty}^{\infty}\int_{-\infty}^{\infty} K_{beam}(x - x_o, y, z - z_o) K_{cap}(x, y, z) \cos(\theta_b) dx dz$$

Sokaras *et al*, Journal of Analytical Atomic Spectroscopy, 2009
Zitnik et *al*, X-Ray Spectrom. 2009, 38, 526–539

Simulation of a pictorial multilayer

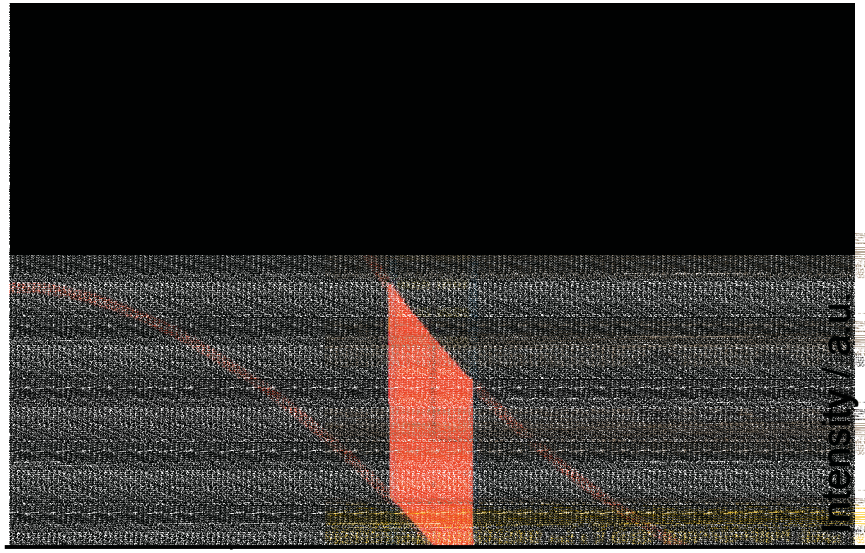

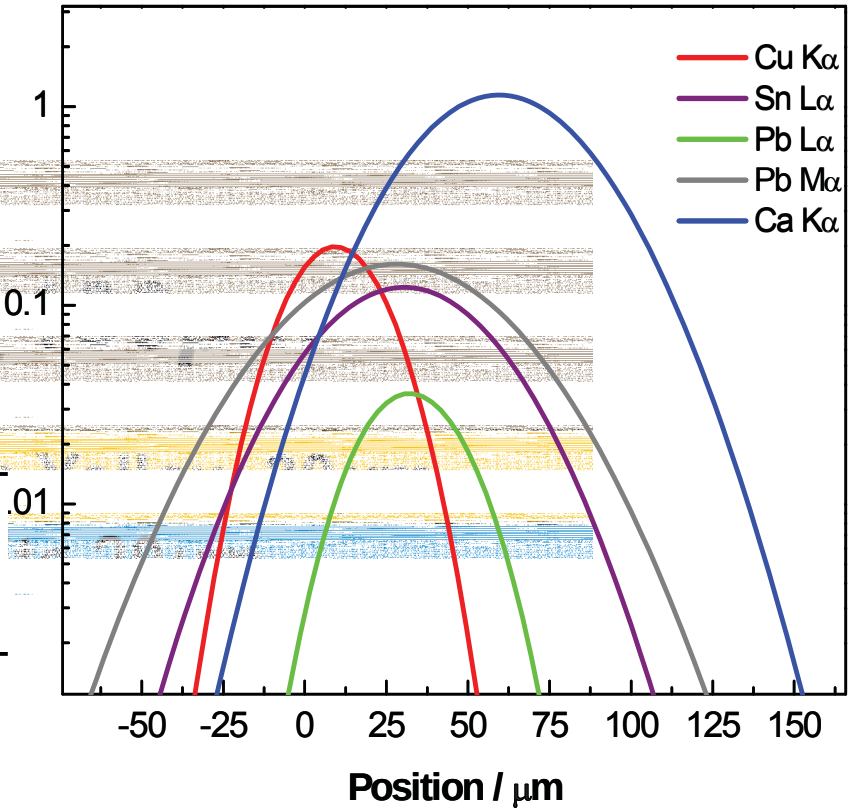

Characteristic	Peak Centroid	Calculation FWHM	System Depth Response FWHM
	m	*m*	*m*
Cu – K_α	9.426	31.97	28.77
Pb – L_α	32.53	35.10	23.91
Pb – M_α	28.19	70.19	68.27
Sn – L_α	30.54	57.97	54.89
Ca – K_α	59.86	56.18	52.36

Depth scanning mode vs 2D Lateral scanning

Advantage of 3D Micro PIXE vs 3D Micro XRF

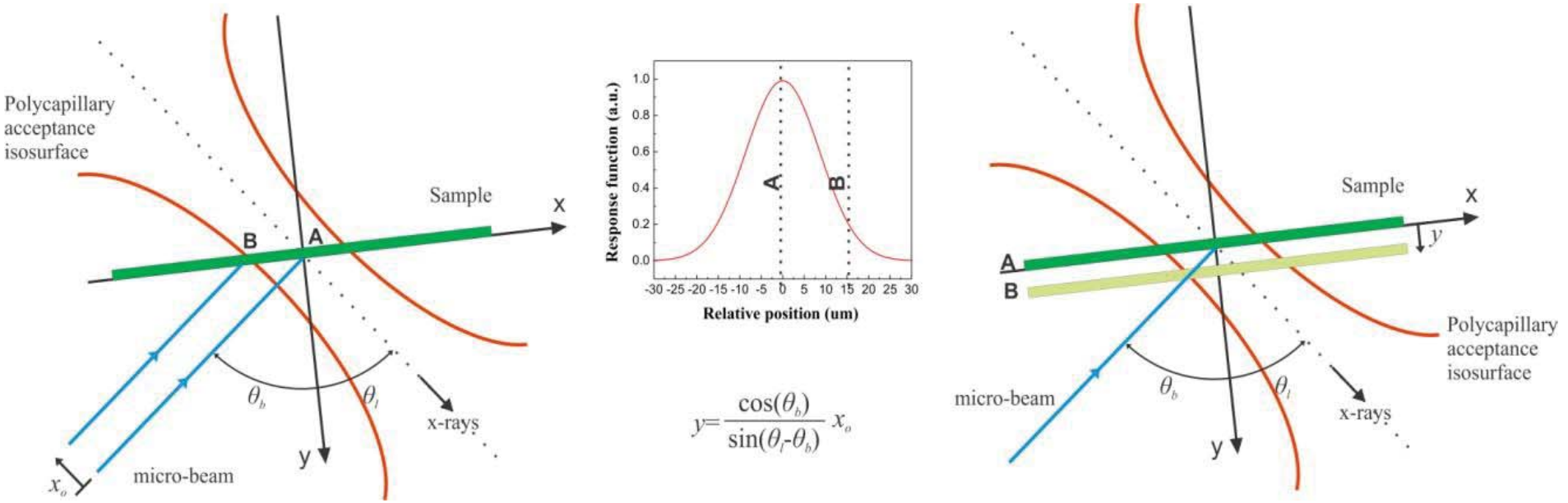

Equivalency of the 2D lateral scanning mode (left hand side) to the sample scanning mode (right hand side).

First 3D Micro-XRF application: Indian Mughal-Paintings 16th – 18th century

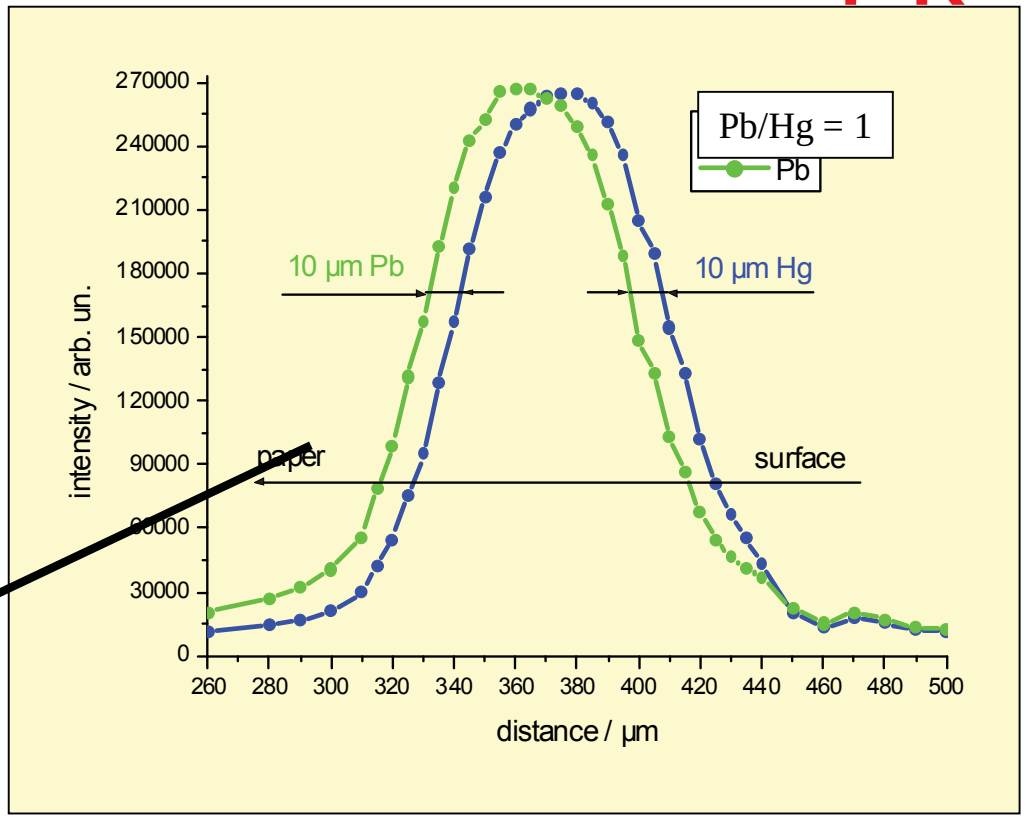

B. Kanngießer, I. Reiche, W. Malzer, NIM B 211, 2003

3D uXRF for Paint layers

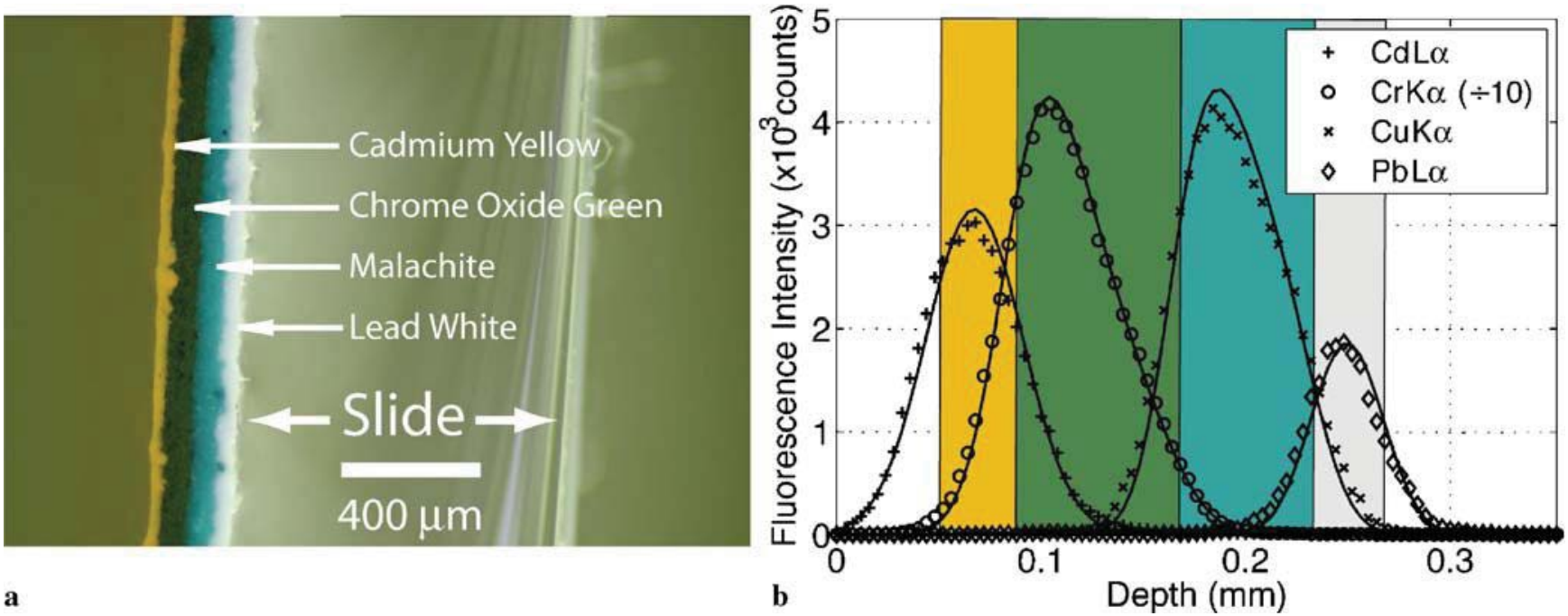

Woll et *al* Appl. Phys. A 83, 235–238 (2006)

Elemental depth profiling of Japanese lacquerware ‘Tamamushi-nuri’

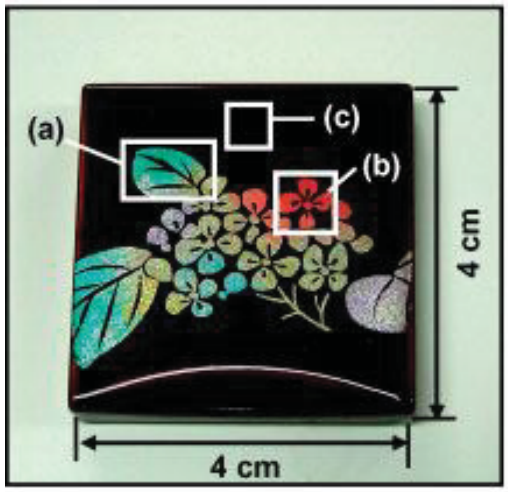

Titan white (TiO_2) as a white pigment.
Cr K lines indicate the presence of green pigment, i.e. chromium oxide (Cr_2O_3) or viridian ($Cr_2O(OH)_4$).
Hg L and S K lines suggest the red pigment of cinnabar (HgS)

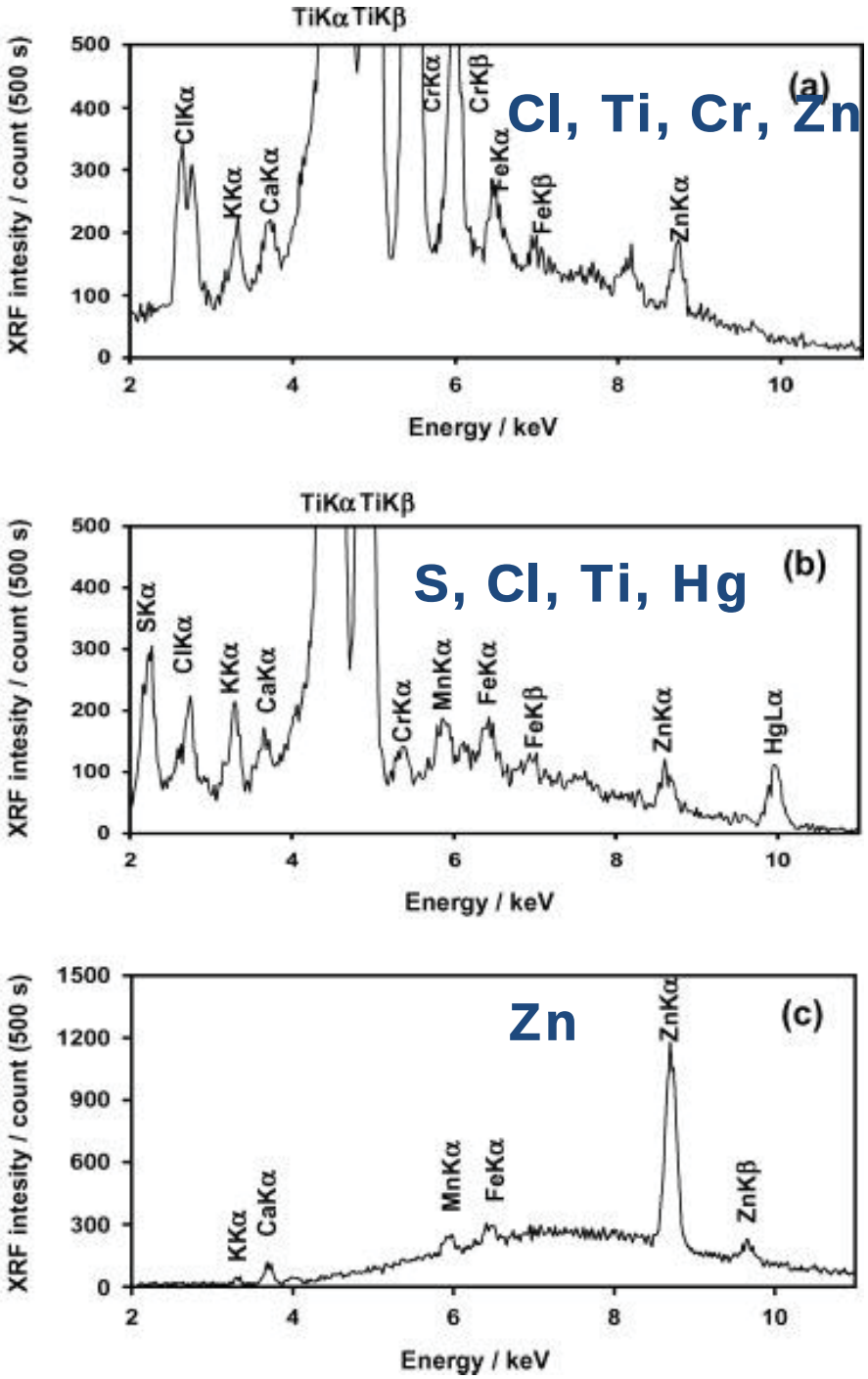

Nakano, Tsuji, XRS 2008, DOI 10.1002/xrs.1163

IAEA

Elemental depth profiling of Japanese lacquerware ‘Tamamushi-nuri’

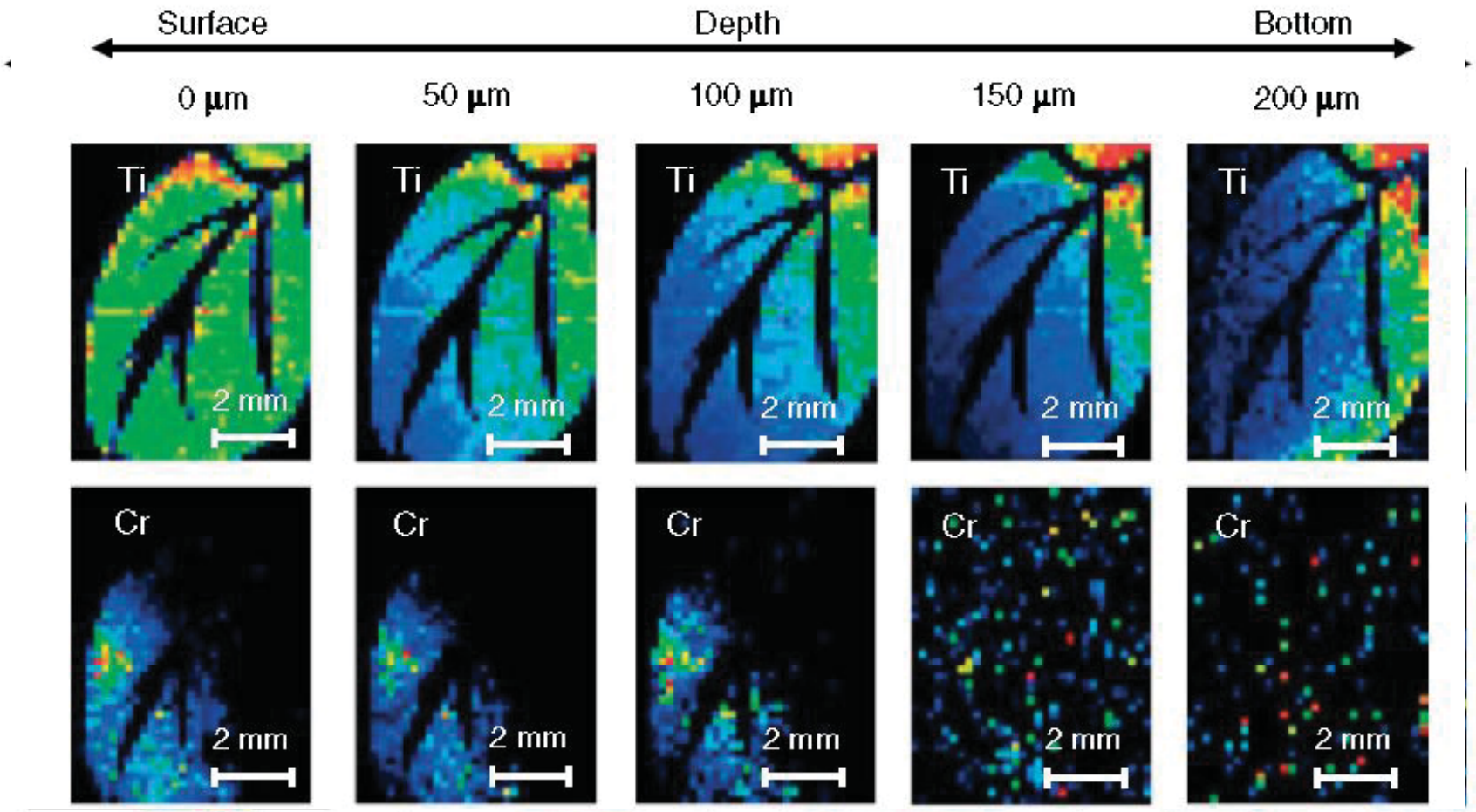

Nakano, Tsuji, XRS 2008, DOI 10.1002/xrs.1163

Elemental depth profiling of Japanese lacquerware ‘Tamamushi-nuri’

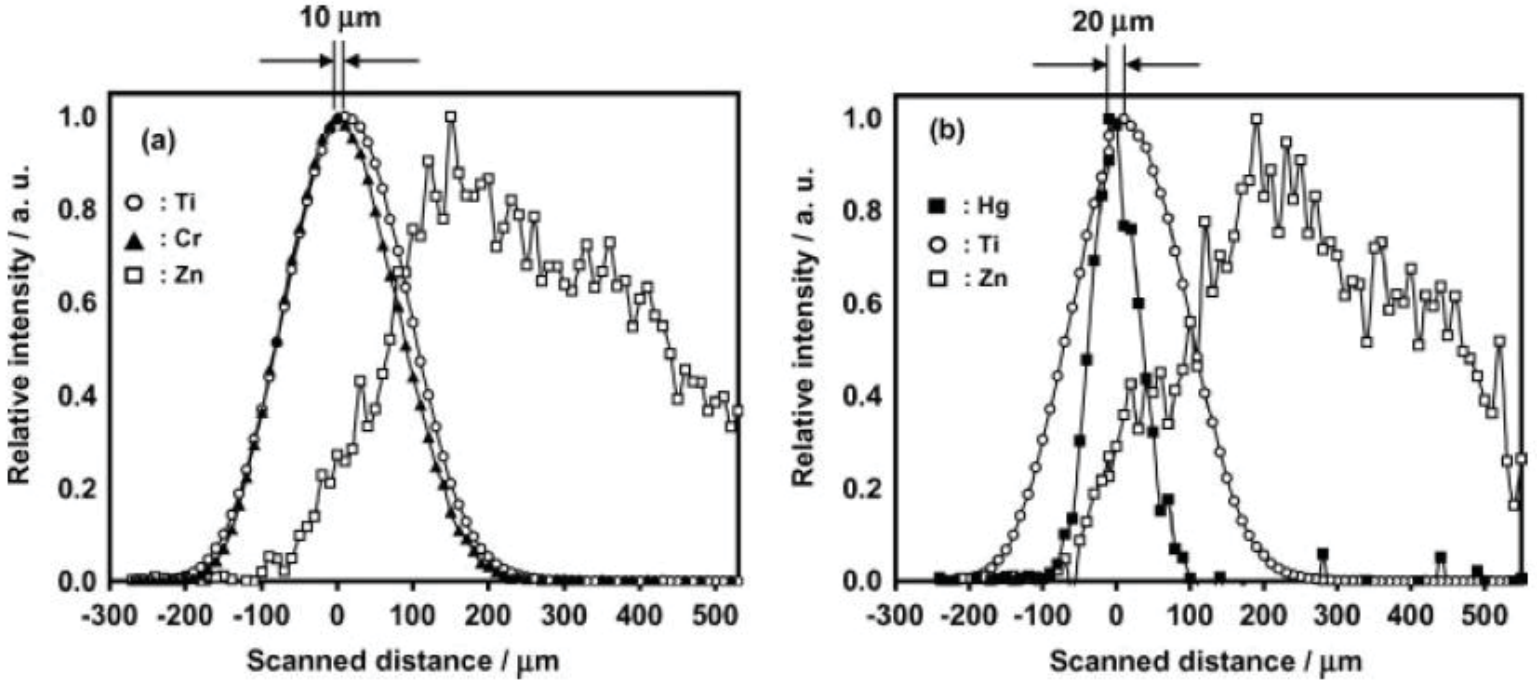

Nakano, Tsuji, XRS 2008, DOI 10.1002/xrs.1163

Max Beckmann's ''Pierrette und Clown'' (1925), in the collection of the Kunsthalle Mannheim, Germany. Oil on canvas 160 X 100 cm

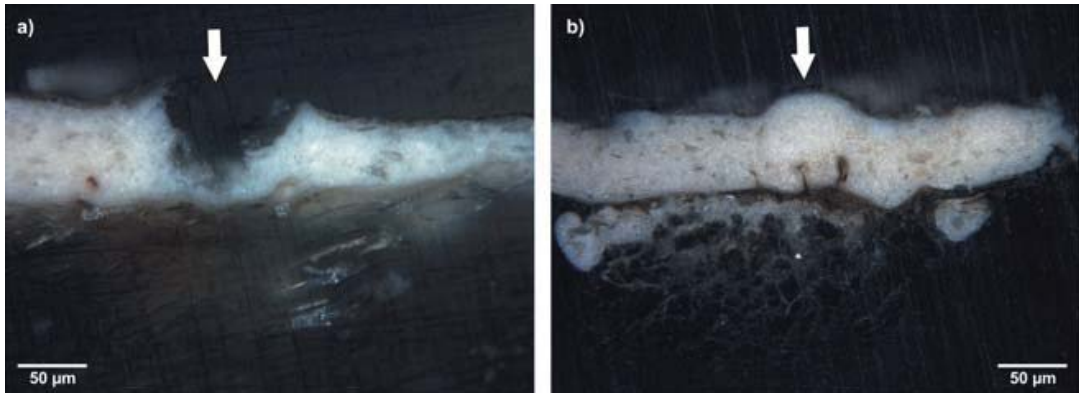

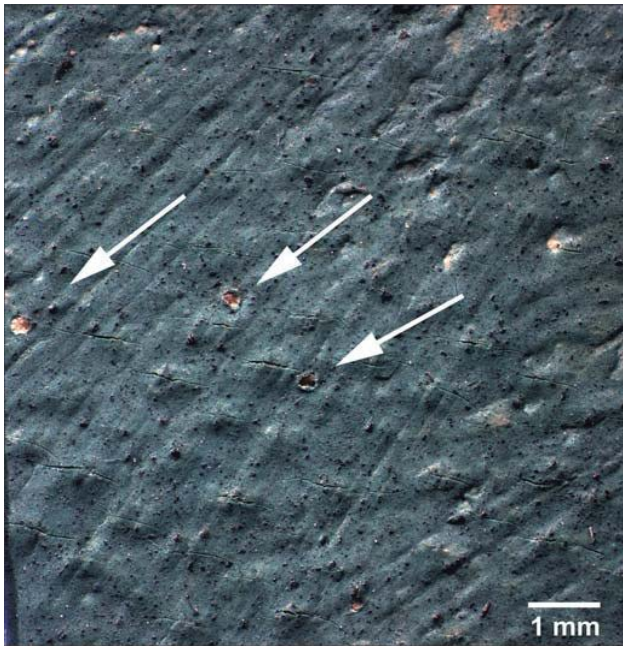

The painting suffers from damage by small protrusions blisters and crater-like holes, filled with metallic soap aggregates

Faubel et al, 2011, JAAS, 10.1039/c0ja00178c

3D XRF on ground layer of Max Beckmann's "Pierrette und Clown" painting

Ground layer from the right side of the painting near the edge of the canvas

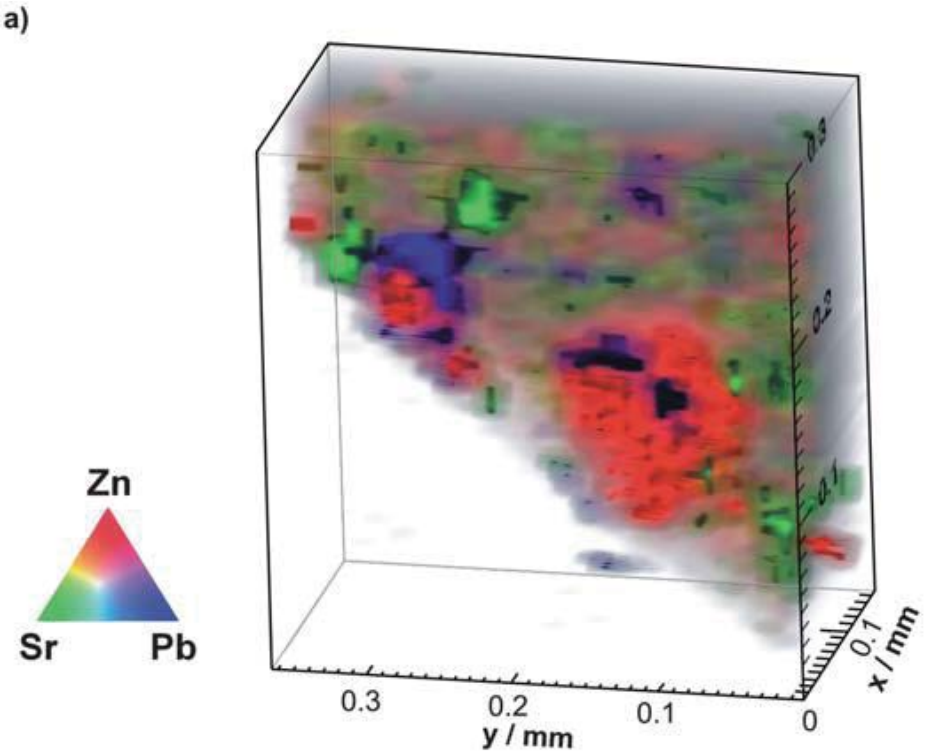

Zinc white + 2fatty acids /zinc soap + water

Competition between Zn stearate and ZnS among

Blisters (both)/protrusions (only Zn stearate) -Raman

IAEA

3D Micro-XRF application:

Reverse painting on glass

- Paint is applied on the glas from the backside – layered system
- Questions posed:
  - Diffusion between paint and glas?
  - Corrosion?
  - Loss of adhesion of the paint!

B. Kanngießer,et al, J. Anal. At. Spectrom., 2008

3D Micro-XRF application (2): Reverse painting on glass

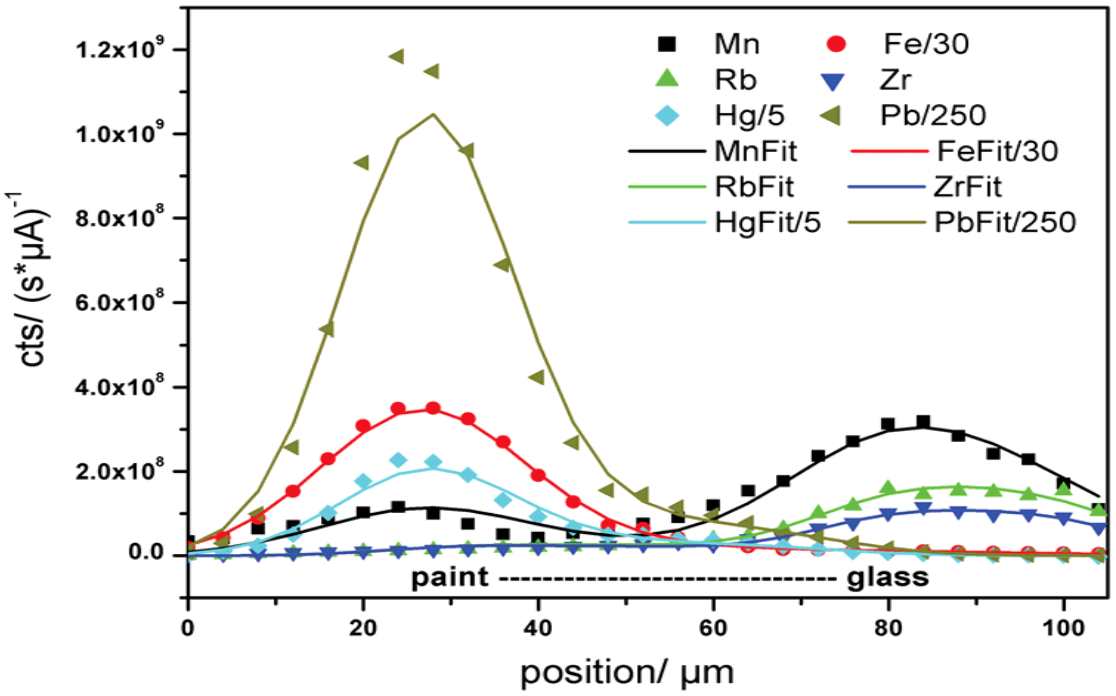

The analysis of the element profiles of Rb and Sr in the diffusion layer provides inferences on the chemical behavior of K and Ca

Scan on blue paint:

- paint layer 7 m, lead white:Berlin blue=5:1, cinnabar
- Corrosion layer (50 m) between paint and glass:
- more Pb, Hg;
- less Mn, Rb, Sr, Zr

3D Micro XRF application (3):
Reverse painting on glass

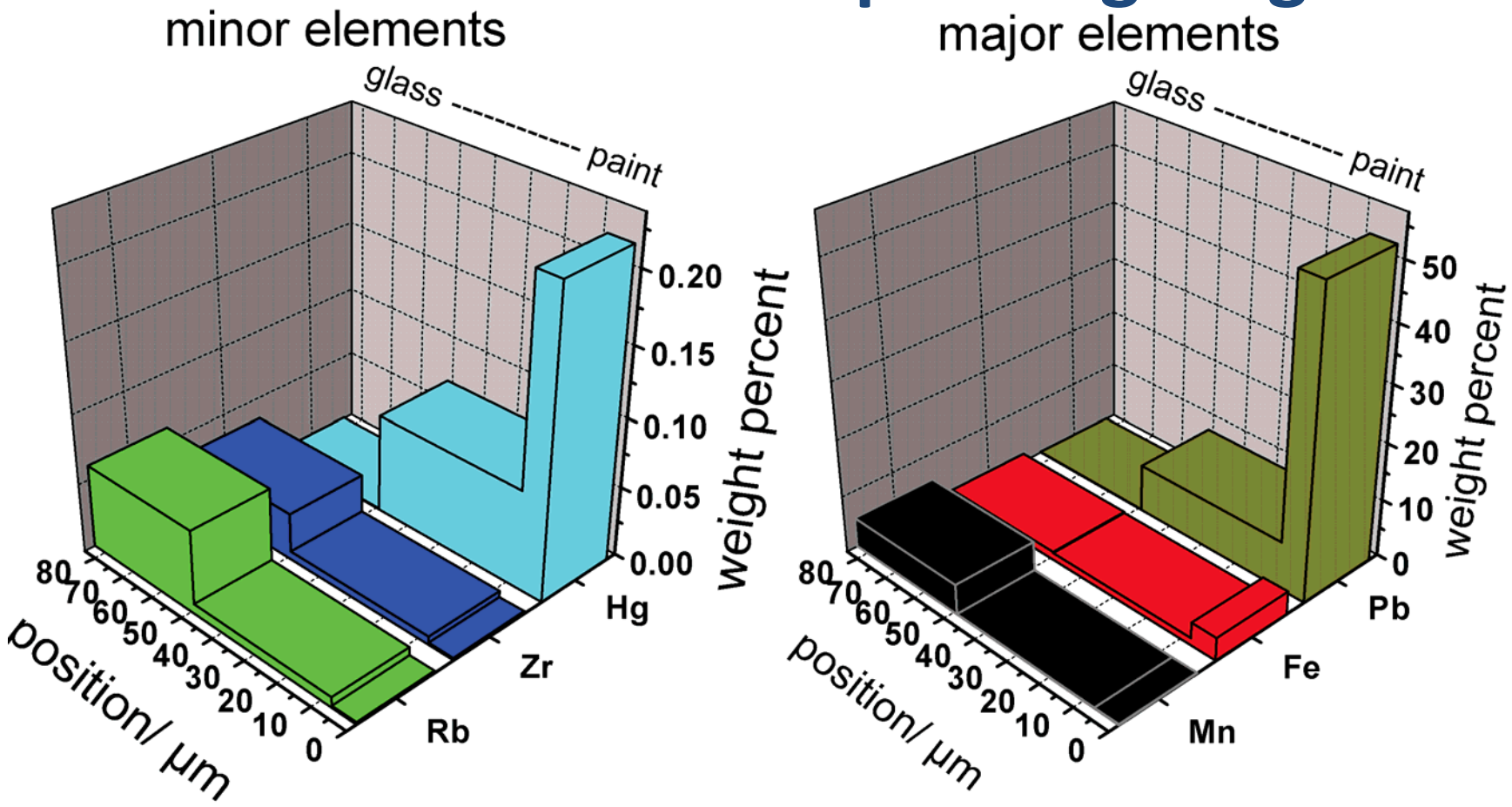

B. Kanngießer,et al, J. Anal. At. Spectrom., 2008

Combined 3D Micro-XRF/2D Micro XRF on the Dead Sea Scrolls

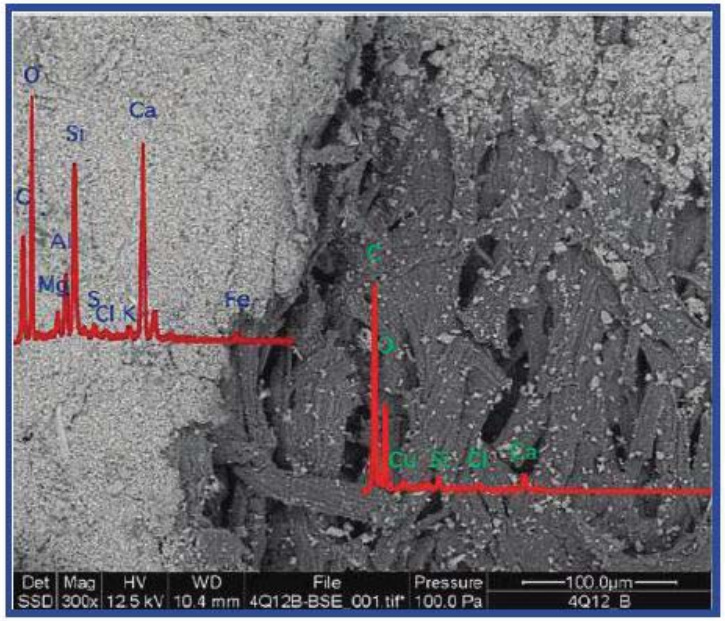

Mantouvalou et al Anal. Chem. 2011, 83, 6308–6315

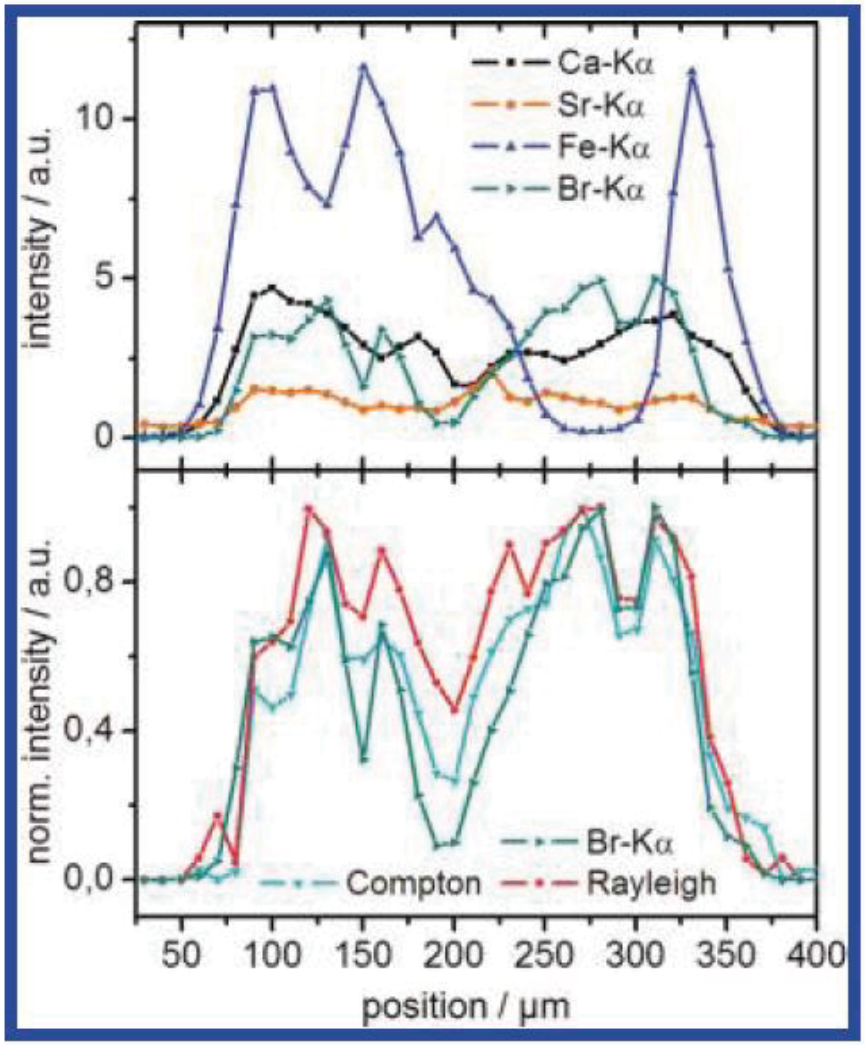

3D analysis of Roman period (2 cent BC) painted plasters @IAEA Laboratories

In support of understanding the elaboration of raw materials and application of painting techniques in antiquity.

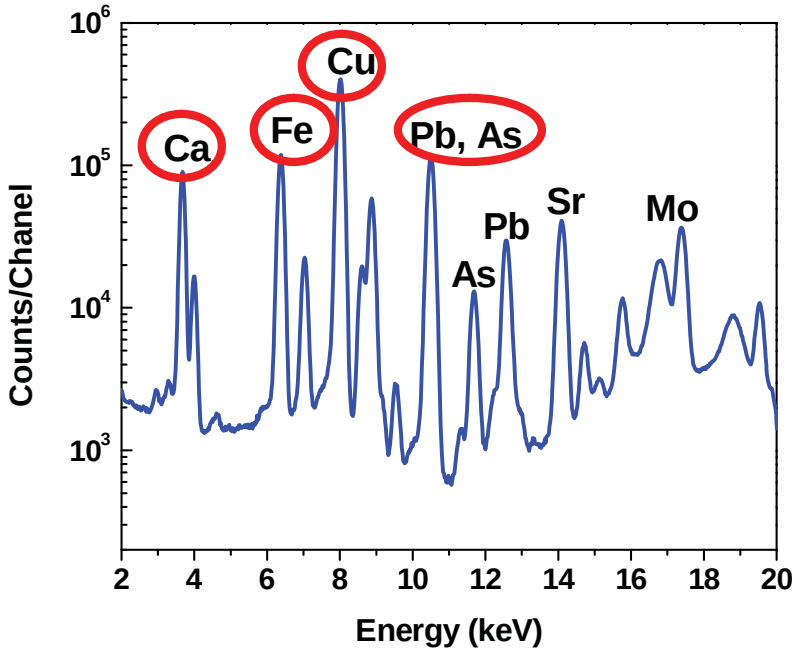

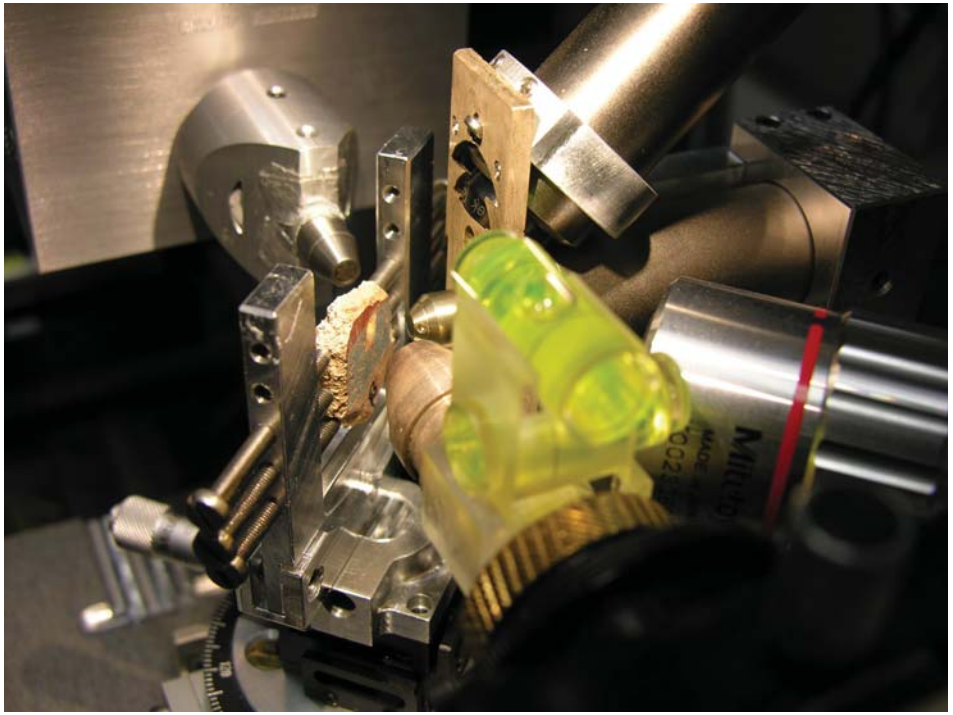

Micro-XRF spectrum from the analysis on extended area

3D analysis of Roman period (2 cent BC) painted plasters @IAEA Laboratories

Egyptian Blue (Cu)
Red ochre (Fe)

Pb and As are constituents trace-minor elements of the iron based ochre paint layer

Volume:
20 m x 1440 m x 293 m,
xyz scanning spacing:
40 m X 40 m x 3 m

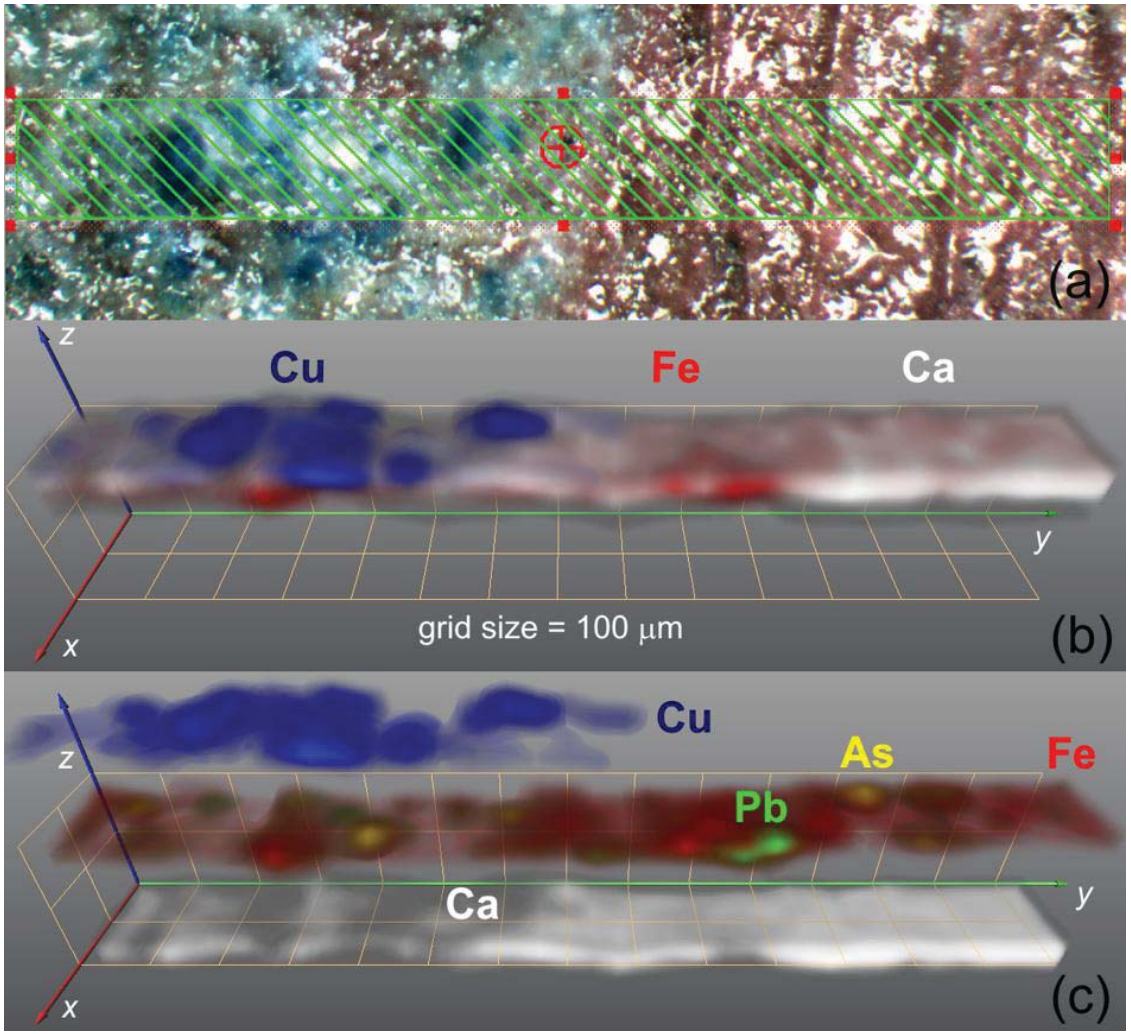

3D Element specific analysis on Aerosol sample

Thick quartz aerosol filters: Pallflex 2500 Q

PM10 collected near **iron-ore** Port terminal, Slovenia.
Microparticles dissolved in quartz fibre filter material
Side micro-PIXE scan; particles distributed up to thickness of 40 um.

Si(Li) detector (polycapillary)

Fe

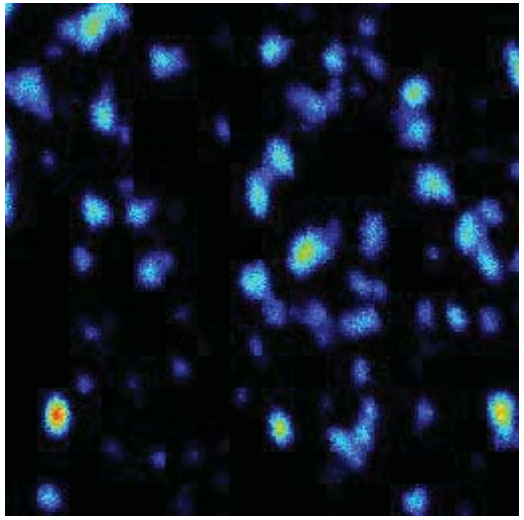

Ge detector (no polycapillary)

Fe

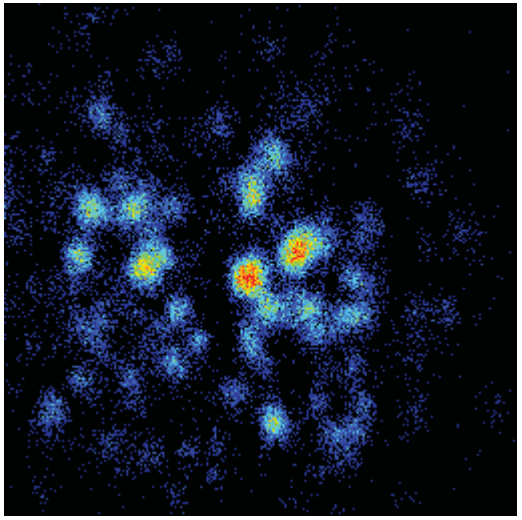

Scan size: 100 µm x 100 µm

3D analysis of Fe rich APM particles

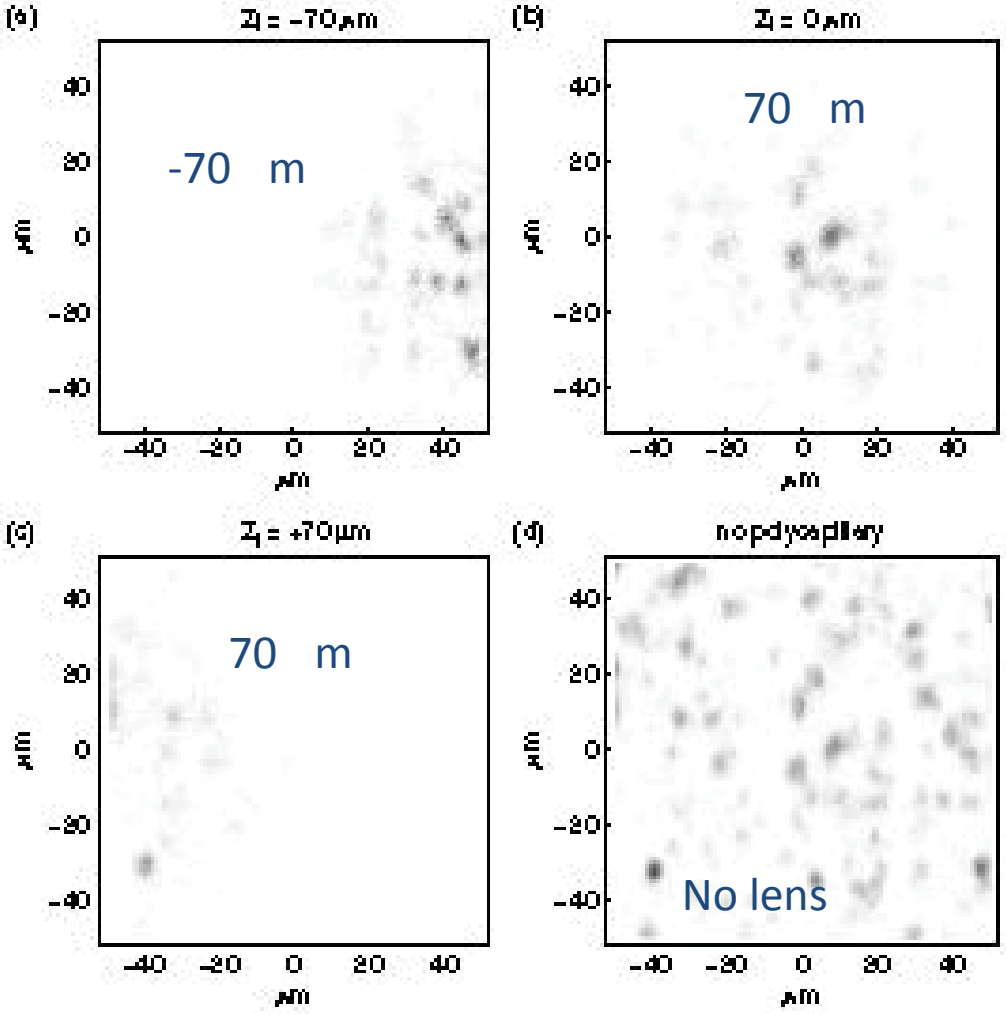

3D analysis of Fe rich APM particles

Scanning area:

100x100 m^2

Filter: Quartz Fibre

Thickness:

5.8mg/cm^2

Steps: 17 x 10 m

➢3D imaging of individual particles

3D-PIXE: Single particle elemental imaging in aerosol filters. Synergy of sample and beam scanning mode

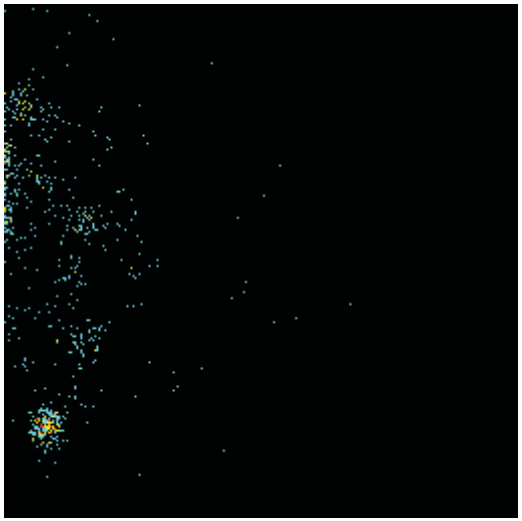

Fe-K_a Mappings

Zitnik, et *al,* Appl. Phys. Lett., 2008
Zitnik et *al*, X-Ray Spectrom. 2009, 38, 526–539

Aerosol particles in quartz filter - Results

Penetration profiles of the strongest x-ray emitters

- Analysis based on Voxels
- Penetration depth of *Fe* is smaller a factor of 2 than the corresponding for *Ca* and *S*.

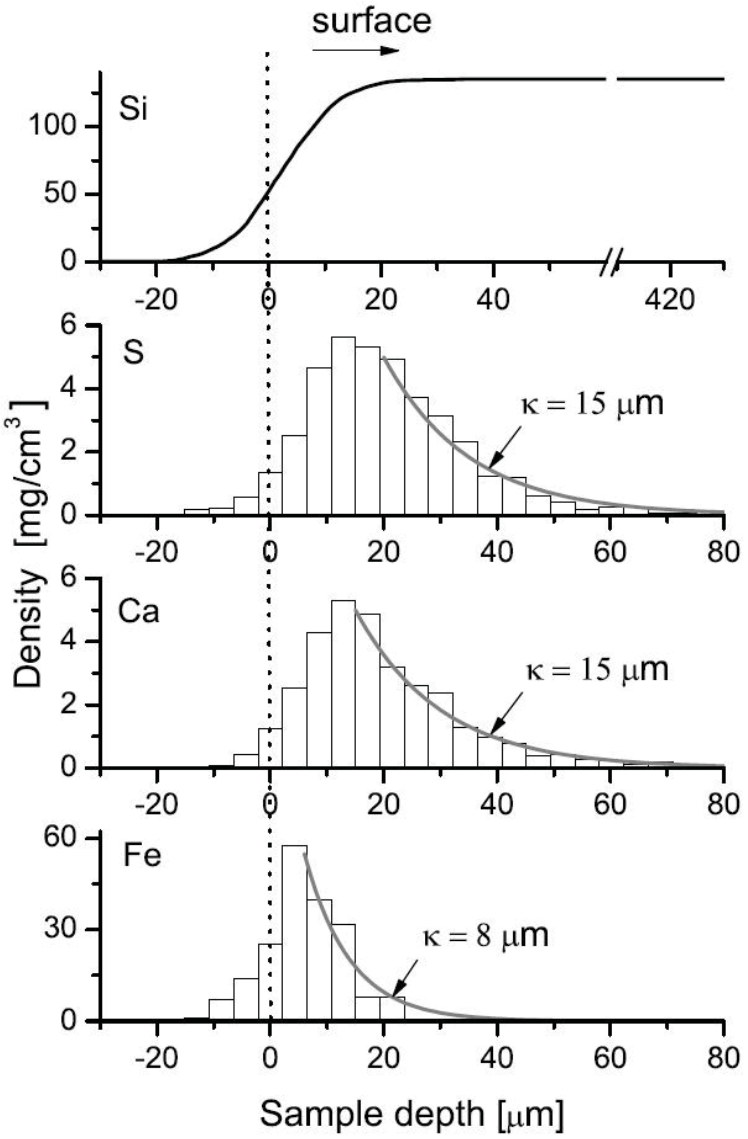

Zitnik, et *al,* Appl. Phys. Lett., 2008
Zitnik et *al*, X-Ray Spectrom. 2009, 38, 526–539

Synopsis/Complementarily

Elements (Alumino-silicate matrix)	Techniques	Probing Depth	Concentration
Na - Cl	3D Micro -PIXE	<10-20 m	Major
K-Zn	3D Micro -PIXE 3D Micro -XRF	<100 m	Major/Minor Major/Minor
Ga – Ag, Au-U Ga - U	3D Micro –PIXE 3D Micro -XRF	<100 m 100-300 m	Major Major/Minor/Trace

3D Micro-XRF: Conclusions

➢The elemental intensity profile incorporates composite analytical information such as the position and height of its centroid, the fwhm or actually the exact shape of the intensity distribution.

3D analysis offers the analytical possibilities:

✓To resolve the elemental distribution in separate layers of a multilayered structure,

✓To determine concentration gradients

3D Micro-PIXE: Conclusions

Special features of 3D Micro-PIXE:

- ✓ One lens
- ✓ Easier alignment – Better overall set-up depth resolution
- ✓ The beam scanning mode provides fast and precise measurements
- ✓ The superior spatial resolution of the exciting beam offers element specific analysis of individual particles at the micrometer scale

Thank you for your attention!